Published for SISSA by Springer

Received: *February 9, 2022*
Revised: *March 22, 2022*
Accepted: *March 24, 2022*
Published: *April 8, 2022*

Study of charmonium and charmonium-like contributions in $B^+ \to J/\psi\eta K^+$ decays

The LHCb collaboration

E-mail: Ivan.Belyaev@itep.ru

Abstract: A study of $B^+ \to J/\psi\eta K^+$ decays, followed by $J/\psi \to \mu^+\mu^-$ and $\eta \to \gamma\gamma$, is performed using a dataset collected with the LHCb detector in proton-proton collisions at centre-of-mass energies of 7, 8 and 13 TeV, corresponding to an integrated luminosity of $9\,fb^{-1}$. The $J/\psi\eta$ mass spectrum is investigated for contributions from charmonia and charmonium-like states. Evidence is found for the $B^+ \to (\psi_2(3823) \to J/\psi\eta)K^+$ and $B^+ \to (\psi(4040) \to J/\psi\eta)K^+$ decays with significance of 3.4 and 4.7 standard deviations, respectively. This constitutes the first evidence for the $\psi_2(3823) \to J/\psi\eta$ decay.

Keywords: B Physics, Branching fraction, Hadron-Hadron Scattering, Quarkonium

ArXiv ePrint: 2202.04045

https://doi.org/10.1007/JHEP04(2022)046

Contents

JHEP04(2022)046

1 Introduction

Exclusive B-meson decays provide an excellent opportunity for studies of charmonium and charmonium-like exotic states. The enigmatic $\chi_{c1}(3872)$ particle, also known as X(3872), was the first discovered charmonium-like state, observed by the Belle collaboration in the $J/\psi\pi^+\pi^-$ mass spectrum from $B^+ \to J/\psi\pi^+\pi^-K^+$ decays [1]. The properties of this state have been extensively studied by the CDF, D0, BaBar, Belle, LHCb, CMS, BESIII and ATLAS collaborations [2–33]. The $\chi_{c1}(3872)$ particle was followed by observations of numerous charmonium-like states [34, 35] that are incompatible with having $c\bar{c}$ quark content, sparking a wave of interest in exotic hadron spectroscopy [35–44]. Despite all theoretical and experimental efforts the nature of such states is not yet understood. For instance, the narrow width of the $\chi_{c1}(3872)$ state and its proximity to the $D^{*0}\overline{D}^0$ mass threshold [29, 30] support the $\chi_{c1}(3872)$ state to be a loosely bound $D^{*0}\overline{D}^0$ molecule [45–51]. Other hypotheses include, but are not limited to, a tetraquark state [52–54], a $c\bar{c}g$ hybrid meson [55], a vector glueball [56], a hadro-charmonium state [57], a cusp [36] or a $\chi_{c1}(2P)$ charmonium state [58, 59]. For some models, the existence of $\chi_{c1}(3872)$ partner states is predicted [52–54, 60–64]. Among these are charged partner $X^\pm$ states and a C-odd partner, referred to hereafter as X'_C state.

The $J/\psi\eta$ final state is well suited to search for the hypothetical X'_C state. Searches for the $X'_C \to J/\psi\eta$ decay have been performed by the BaBar and Belle collaborations using $B^+ \to J/\psi\eta K^+$ decays [65, 66]. No $X'_C \to J/\psi\eta$ signal is observed, and upper limits at 90% confidence level (CL) on the product of branching fractions for the $B^+ \to X'_C K^+$ and $X'_C \to J/\psi\eta$ decays are set to be 7.7×10^{-6} (BaBar) and 3.8×10^{-6} (Belle).

In this paper a study of the J/ψη mass spectrum from $B^+ \to J/\psi\eta K^+$ decays[1] is reported. In particular searches for contributions from new hypothetical states, denoted hereafter as X, or known charmonia or charmonium-like resonances are performed. The study uses a dataset collected with the LHCb detector at 7, 8 and 13 TeV centre-of-mass energies corresponding to an integrated luminosity of $9\,\text{fb}^{-1}$. The results are reported in the form of a ratio of branching fractions using the normalisation decay mode $B^+ \to (\psi(2S) \to J/\psi\eta)\, K^+$,

$$F_X \equiv \frac{\mathcal{B}(B^+ \to XK^+) \times \mathcal{B}(X \to J/\psi\eta)}{\mathcal{B}(B^+ \to \psi(2S)K^+) \times \mathcal{B}(\psi(2S) \to J/\psi\eta)}\,, \tag{1.1}$$

and as the product of branching fractions

$$B_X \equiv \mathcal{B}(B^+ \to XK^+) \times \mathcal{B}(X \to J/\psi\eta)\,, \tag{1.2}$$

the latter obtained from the F_X ratio using the known values of the $B^+ \to \psi(2S)K^+$ and $\psi(2S) \to J/\psi\eta$ branching fractions [34, 65, 66]. The results are obtained for masses of the hypothetical X state in the region between the J/ψη threshold and $4.65\,\text{GeV}/c^2$. The F_X ratio and the product of branching fractions B_X are also measured for the ψ(3770), $\psi_2(3823)$ [30], $\psi_3(3842)$ [67], ψ(4040), ψ(4160), ψ(4415) charmonium states [34], as well as the charmonium-like R(3760), R(3790) [68], $Z_c(3900)^0$ [69, 70], ψ(4230) [71], ψ(4360) [72–74] and ψ(4390) states [75, 76], the hypothetical neutral partner of the charged $Z_c(4430)^+$ state [77–81], referred to as $Z_c(4430)^0$ hereafter, and finally for the X'_C state.

2 Detector and simulation

The LHCb detector [82, 83] is a single-arm forward spectrometer covering the pseudorapidity range $2 < \eta < 5$, designed for the study of particles containing b or c quarks. The detector includes a high-precision tracking system consisting of a silicon-strip vertex detector surrounding the proton-proton (pp) interaction region, a large-area silicon-strip detector located upstream of a dipole magnet with a bending power of about 4 Tm, and three stations of silicon-strip detectors and straw drift tubes placed downstream of the magnet. The tracking system provides a measurement of the momentum, p, of charged particles with a relative uncertainty that varies from 0.5% at low momentum to 1.0% at $200\,\text{GeV}/c$. The minimum distance of a track to a primary pp collision vertex (PV), the impact parameter, is measured with a resolution of $(15 + 29/p_T)\,\mu\text{m}$, where p_T is the component of the momentum transverse to the beam, in GeV/c. Different types of charged hadrons are distinguished using information from two ring-imaging Cherenkov detectors. Photons, electrons and hadrons are identified by a calorimeter system consisting of scintillating-pad and preshower detectors, an electromagnetic and a hadronic calorimeter [84]. Muons are identified by a system composed of alternating layers of iron and multiwire proportional chambers.

The online event selection is performed by a trigger, which consists of a hardware stage, based on information from the calorimeter and muon systems, followed by a software stage, which applies a full event reconstruction. At the hardware trigger stage, events are

[1] Inclusion of charge-conjugate states is implied throughout the paper.

JHEP04(2022)046

required to have a muon with high transverse momentum or dimuon candidates in which the product of the p_{T} of the muons has a high value. In the software trigger, two oppositely charged muons are required to form a good-quality vertex that is significantly displaced from every PV, with a dimuon mass exceeding $2.7\,\mathrm{GeV}/c^2$.

Simulated events are used to describe signal shapes and to compute the efficiencies needed to determine the branching fraction ratios. In the simulation, pp collisions are generated using Pythia [85] with a specific LHCb configuration [86]. Decays of unstable particles are described by EvtGen [87], in which final-state radiation is generated using Photos [88]. The interaction of the generated particles with the detector, and its response, are implemented using the Geant4 toolkit [89, 90] as described in ref. [91]. The transverse momentum and rapidity, y, spectra of the B^+ mesons in simulation are corrected to represent better those observed in data. The correction factors are calculated by comparing the observed p_{T} and y spectra for a high-yield and low-background sample of reconstructed $\mathrm{B}^+ \to \mathrm{J}/\psi\mathrm{K}^+$ decays with corresponding simulated samples. In the simulation, the $\mathrm{B}^+ \to \mathrm{J}/\psi\eta\mathrm{K}^+$ decays are produced according to a phase-space decay model. Simulated decays are corrected to reproduce the $\mathrm{J}/\psi\eta$ and $\eta\mathrm{K}^+$ mass distributions observed in data. To describe accurately the variables used for kaon identification, the corresponding quantities in simulation are resampled according to values obtained from calibration data samples of $\mathrm{D}^{*+} \to (\mathrm{D}^0 \to \mathrm{K}^-\pi^+)\,\pi^+$ decays [92]. The procedure accounts for correlations between the variables associated to a particular track, as well as the dependence of the kaon identification response on p_{T}, η and the multiplicity of tracks in the event. To account for imperfections in the simulation of charged-particle reconstruction, the track reconstruction efficiency determined from simulation is corrected using control channels in data [93].

3 Event selection

Candidate $\mathrm{B}^+ \to \mathrm{J}/\psi\eta\mathrm{K}^+$ decays are reconstructed through the $\mathrm{J}/\psi \to \mu^+\mu^-$ and $\eta \to \gamma\gamma$ decay modes. A loose initial selection is applied to reduce the background. The criteria are chosen to be similar to those used in previous LHCb studies [21, 94–98]. Subsequently, a multivariate estimator based on an artificial neural network algorithm [99, 100], configured with a cross-entropy cost estimator [101], in the following referred to as the MLP classifier, is applied.

Muon and kaon candidates are identified by combining information from the Cherenkov detectors, calorimeters and muon detectors [102] associated to the reconstructed tracks. Transverse momenta of muon candidates are required to be greater than $550\,\mathrm{MeV}/c$. To reduce combinatorial background only tracks that are inconsistent with originating from any reconstructed PV in the event are considered. Pairs of oppositely charged muons consistent with originating from a common vertex are combined to form $\mathrm{J}/\psi \to \mu^+\mu^-$ candidates. The reconstructed mass of the pair is required to be between 3.056 and $3.136\,\mathrm{GeV}/c^2$.

Photons are reconstructed from clusters in the electromagnetic calorimeter that have transverse energy larger than 500 MeV and are not associated with reconstructed tracks [84, 103]. Photon identification is based on the combined information from electromagnetic and hadronic calorimeters, scintillation pad and preshower detectors and

JHEP04(2022)046

the tracking system. Candidate $\eta \to \gamma\gamma$ decays are reconstructed as diphoton combinations with mass within ± 60 MeV/c^2 of the known η mass [34] and transverse momentum greater than 1.5 GeV/c.

The selected J/ψ candidates are combined with K^+ and η candidates to form B^+ candidates. Each B^+ candidate is associated with the PV that yields the smallest $\chi^2_{\rm IP}$, where $\chi^2_{\rm IP}$ is defined as the difference in the vertex-fit χ^2 of a given PV reconstructed with and without the charged tracks that form the B^+ candidate under consideration. To improve the B^+ mass resolution a kinematic fit [104] is performed. This fit constrains the $\mu^+\mu^-$ and $\gamma\gamma$ masses to the known J/ψ and η mesons masses [34], respectively, and the B^+ candidate to originate from its associated PV. The proper decay time of the B^+ candidate is required to be greater than 200 μm/c to suppress the large combinatorial background.

A further selection based on the MLP classifier reduces the combinatorial background to a low level whilst retaining a high signal efficiency. Variables included in the classifier are related to the reconstruction quality, kinematics and decay time of the B^+ candidates, kinematics of the final-state particles and a variable that characterises kaon identification. The classifier is trained using simulated samples of $B^+ \to J/\psi\eta K^+$ decays as signal proxy. The $B^+ \to J/\psi\eta K^+$ candidates from data with mass, $m_{J/\psi\eta K^+}$, ranging between 5.4 and 5.7 GeV/c^2, are used as background proxy. To avoid introducing a bias in the MLP evaluation due to overfitting, a k-fold cross-validation technique [105] with $k = 13$ is used.

The requirement on the MLP classifier is chosen to maximize the figure-of-merit defined as $S/\sqrt{B+S}$, where S represents the expected signal yield from simulation, and B stands for the background yield obtained by fitting the data. The expected signal yield is estimated as $S = \varepsilon S_0$, where ε is the efficiency of the requirement on the MLP classifier determined from simulation, and S_0 is the signal yield obtained from the fit to the data when no requirement is applied. The mass distribution of selected $B^+ \to J/\psi\eta K^+$ candidates is shown in figure 1.

4 $B^+ \to J/\psi\eta K^+$ signal and J/$\psi\eta$ mass spectrum

The $B^+ \to J/\psi\eta K^+$ signal yield is determined using an extended unbinned maximum-likelihood fit to the $J/\psi\eta K^+$ mass distribution with signal and background components. The signal is modelled by a modified Gaussian function with power-law tails on both sides of the distribution [106, 107], referred to hereafter as $\mathcal{F}_{\mathcal{S}}$. The tail parameters of the modified Gaussian function are fixed from simulation, while the peak position and resolution are allowed to vary in the fit. The combinatorial background is parametrised with an exponential function. The fit result is overlaid in figure 1 and the signal yield is found to be

$$N_{B^+\to J/\psi\eta K^+} = (5.39 \pm 0.16) \times 10^3 \,.$$

The search for the $B^+ \to (X \to J/\psi\eta) K^+$ signal is performed using extended unbinned maximum-likelihood fits to the background-subtracted J/$\psi\eta$ mass spectrum. The *sPlot* technique [108] is used for the background subtraction using the $J/\psi\eta K^+$ mass as the discriminating variable. To improve the J/$\psi\eta$ mass resolution and to eliminate a small correlation between the $m_{J/\psi\eta K^+}$ and $m_{J/\psi\eta}$ variables, the J/$\psi\eta$ mass is computed using a kinematic fit [104]

JHEP04(2022)046

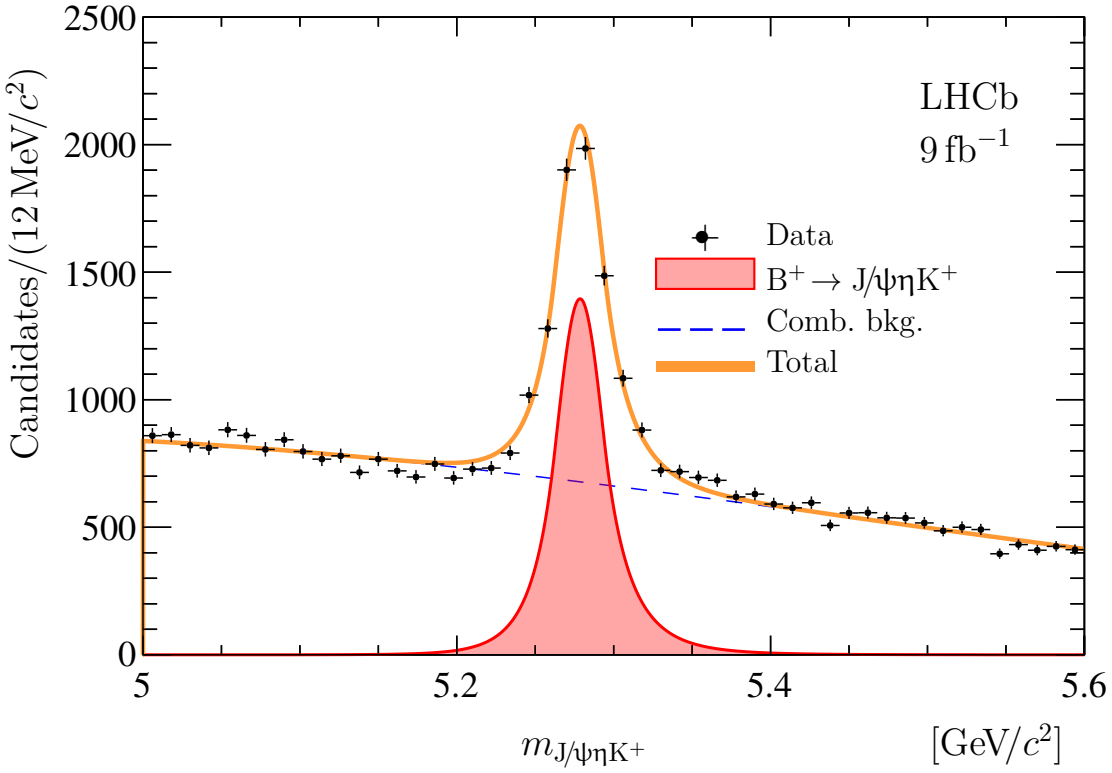

Figure 1. Mass distribution of selected $B^+ \to J/\psi\eta K^+$ candidates. The result of the fit, described in the text, is overlaid.

that constrains the mass of the B^+ candidate to its known value [34]. For easier parametrisation of the nonresonant component, the fit to the $J/\psi\eta$ mass distribution is performed separately in four different overlapping mass regions. For X masses below 3.875 GeV/c^2, a fit of the lowest-mass region, $3.65 < m_{J/\psi\eta} < 3.90$ GeV/c^2, is performed. The $J/\psi\eta$ mass regions $3.85 < m_{J/\psi\eta} < 4.05$ GeV/c^2, $4.0 < m_{J/\psi\eta} < 4.2$ GeV/c^2, and $4.15 < m_{J/\psi\eta} < 4.70$ GeV/c^2 are used for X masses within the ranges $3.875 < m_X < 4.025$ GeV/c^2, $4.025 < m_X < 4.175$ GeV/c^2, and $4.175 < m_X < 4.675$ GeV/c^2, respectively. The background-subtracted $J/\psi\eta$ mass distribution for these regions is shown in figure 2. A clear narrow peak, corresponding to the $B^+ \to (\psi(2S) \to J/\psi\eta) K^+$ decay, is visible in the low-mass region. This signal is used as a normalisation channel.

The fit function to the lowest-mass region consists of three components:

1. the decay of interest $B^+ \to (X \to J/\psi\eta) K^+$, referred to as $\mathcal{C}_X$ component;
2. the $B^+ \to (\psi(2S) \to J/\psi\eta) K^+$ signal, referred to as $\mathcal{C}_{\psi(2S)}$ component;
3. the $B^+ \to (J/\psi\eta)_{NR} K^+$ decays with no resonances in the $J/\psi\eta$ system, and referred to as $\mathcal{C}_{NR}$ component.

The $\mathcal{C}_{\psi(2S)}$ component and the $\mathcal{C}_X$ contribution for X states with the natural width negligible with respect to the detector resolution (referred as narrow) are modelled using the $\mathcal{F}_S$ shape.

JHEP04(2022)046

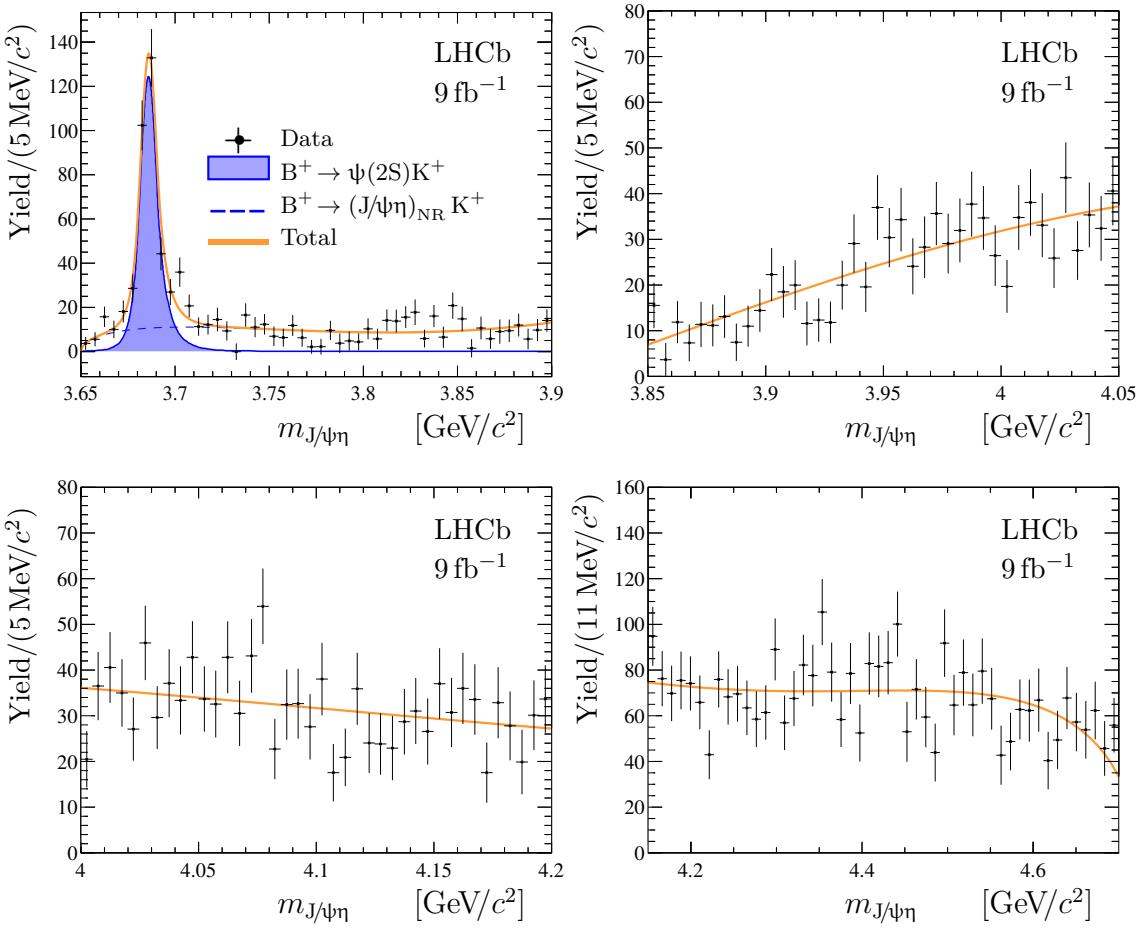

Figure 2. Background-subtracted J/ψη mass distribution from $B^+ \to J/\psi\eta K^+$ decays in four J/ψη mass regions. The results of the fits without contributions from a narrow X state, described in the text, are overlaid.

The tail parameters of all the $\mathcal{F}_S$ functions are fixed from simulation, while the peak position and resolution parameter for the $\mathcal{C}_{\psi(2S)}$ component are allowed to vary in the fit. The ratio of the resolution parameters for the $\mathcal{C}_X$ and $\mathcal{C}_{\psi(2S)}$ components is fixed at the value obtained from simulation. This procedure also accounts for a small imperfection in the modelling of the J/ψη mass resolution in the simulation [29, 30, 33]. The nonresonant component $\mathcal{C}_{NR}$ is parameterised with a product of the phase-space function describing a two-body system out of the three-body final state [109] and a positive first-order polynomial function.

For X masses above 3.875 GeV/c^2, the fit is performed simultaneously in two J/ψη mass regions, one containing the X mass and the other the ψ(2S) state. For the X mass region the fit function consists of a pair of components, $\mathcal{C}_X$ and $\mathcal{C}_{NR}$, while the ψ(2S) region fit includes the $\mathcal{C}_{\psi(2S)}$ and $\mathcal{C}_{NR}$ components. The parameters for two $\mathcal{C}_{NR}$ components are independent in the two regions.

No significant signal is found for $B^+ \to (X \to J/\psi\eta)\, K^+$ decays occurring via a hypothetical narrow X particle in the $3.7 < m_X < 4.7$ GeV/c^2 mass region. Fit results without the $\mathcal{C}_X$ component are shown in figure 2, illustrating that no sizeable contribution from decays

JHEP04(2022)046

with a narrow intermediate X state is required to describe the data. To quantify the absence of the $\mathrm{B}^+ \to (\mathrm{X} \to \mathrm{J}/\psi\eta)\,\mathrm{K}^+$ signal, fits are performed with the mass m_X of the hypothetical X particle fixed to a value that is scanned across the whole available $\mathrm{J}/\psi\eta$ mass range. The yield of the $\mathcal{C}_\mathrm{X}$ component, N_X, is parametrised using the yield of the $\mathcal{C}_{\psi(2\mathrm{S})}$ component, $N_{\psi(2\mathrm{S})}$, and the ratio of branching fractions, F_X, defined by eq. (1.1), as

$$N_\mathrm{X}(m_\mathrm{X}) = N_{\psi(2\mathrm{S})} F_\mathrm{X}(m_\mathrm{X}) R_\varepsilon(m_\mathrm{X})\,, \tag{4.1a}$$

where R_ε is the ratio of total efficiencies for the $\mathrm{B}^+ \to (\mathrm{X} \to \mathrm{J}/\psi\eta)\,\mathrm{K}^+$ and $\mathrm{B}^+ \to (\psi(2\mathrm{S}) \to \mathrm{J}/\psi\eta)\,\mathrm{K}^+$ channels, described in section 5. The parameters $N_{\psi(2\mathrm{S})}$ and F_X are left to vary in the fit, and the uncertainty on the ratio R_ϵ is included in the fit through a Gaussian constraint. A second set of fits exploits an alternative parametrisation that allows for the determination of the product of the branching fractions B_X, defined by eq. (1.2), through

$$N_\mathrm{X}(m_\mathrm{X}) = \frac{N_{\psi(2\mathrm{S})} B_\mathrm{X}(m_\mathrm{X}) R_\varepsilon(m_\mathrm{X})}{\mathcal{B}\left(\mathrm{B}^+ \to \psi(2\mathrm{S})\mathrm{K}^+\right) \mathcal{B}\left(\psi(2\mathrm{S}) \to \mathrm{J}/\psi\eta\right)}\,, \tag{4.1b}$$

where $N_{\psi(2\mathrm{S})}$ and B_X are fit parameters, and uncertainties for the branching fractions $\mathcal{B}\left(\mathrm{B}^+ \to \psi(2\mathrm{S})\mathrm{K}^+\right)$ and $\mathcal{B}\left(\psi(2\mathrm{S}) \to \mathrm{J}/\psi\eta\right)$ [34] are included in the fit using Gaussian constraints.

In addition to the search for decays with a narrow hypothetical X state, a search is performed for decays mediated by known conventional charmonium or charmonium-like states, including the hypothetical X'_C state and the neutral partner of the $\mathrm{Z_c}(4430)^+$ state. For the latter it is assumed that the mass and width are the same as for its charged partner [77–81], while for the X'_C state the mass and width are assumed to be the same as for the $\chi_{\mathrm{c}1}(3872)$ state [29, 30]. The $\mathcal{C}_\mathrm{X}$ component is parametrised with a relativistic S-wave Breit-Wigner shape convolved with the $\mathcal{F}_S$ function. For each resonance with a mass larger than $3.9\,\mathrm{GeV}/c^2$ a fit range is chosen individually depending on the resonance mass and width. The uncertainties on the resonance parameters are included in the fits using Gaussian constraints. For the $\psi_2(3823)$ state, where only the upper limit for the natural width is known [30], a natural width of 1 MeV is assumed. The background-subtracted $\mathrm{J}/\psi\eta$ mass spectra in the corresponding ranges, together with the fit results, are shown in figures 3 to 5. For the $\mathrm{B}^+ \to (\psi_2(3823) \to \mathrm{J}/\psi\eta)\,\mathrm{K}^+$ and $\mathrm{B}^+ \to (\psi(4040) \to \mathrm{J}/\psi\eta)\,\mathrm{K}^+$ decays, signals with a statistical significance of 3.4 and 9.0 standard deviations, respectively, are seen. No evidence for other decays is obtained.

5 Efficiency and systematic uncertainty

For each considered value of m_X, the efficiency ratio R_ε from eq. (4.1a) is calculated as

$$R_\varepsilon(m_\mathrm{X}) \equiv \frac{\varepsilon(\mathrm{B}^+ \to (\mathrm{X} \to \mathrm{J}/\psi\eta)\,\mathrm{K}^+)}{\varepsilon(\mathrm{B}^+ \to (\psi(2\mathrm{S}) \to \mathrm{J}/\psi\eta)\,\mathrm{K}^+)}\,, \tag{5.1}$$

where the total efficiency ε for each decay is calculated from the product of the detector acceptance, the reconstruction and selection efficiencies for decays within the detector

JHEP04(2022)046

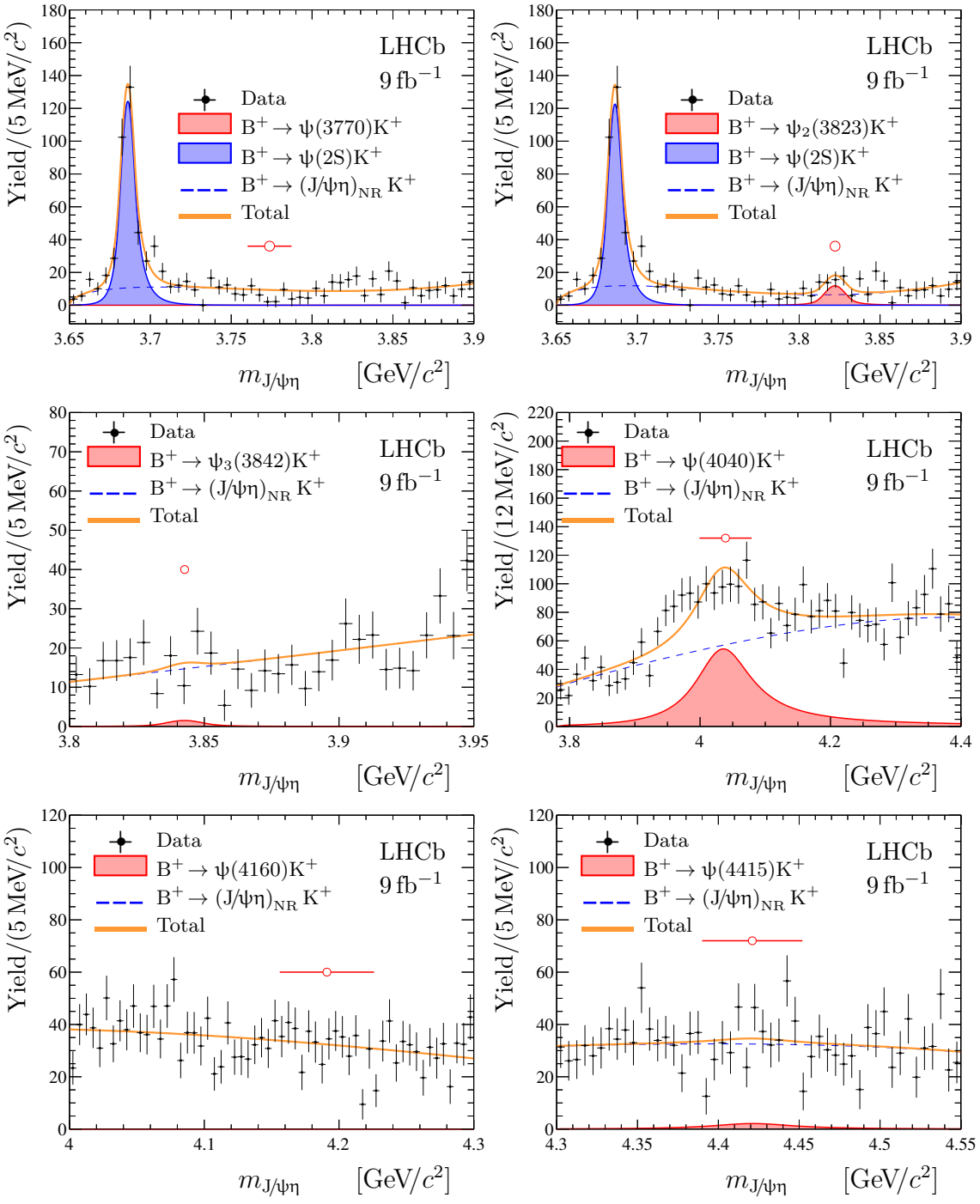

Figure 3. Background-subtracted J/ψη mass distribution from $B^+ \to J/\psi\eta K^+$ decays in the vicinity of the conventional (top row) ψ(3770), $\psi_2(3823)$, (middle row) $\psi_3(3842)$, ψ(4040), (bottom row) ψ(4160) and ψ(4415) charmonium states. The results of the fits, described in the text, are overlaid. The red open point with horizontal error bars indicates the mass and width of the resonance assumed in the fits.

JHEP04(2022)046

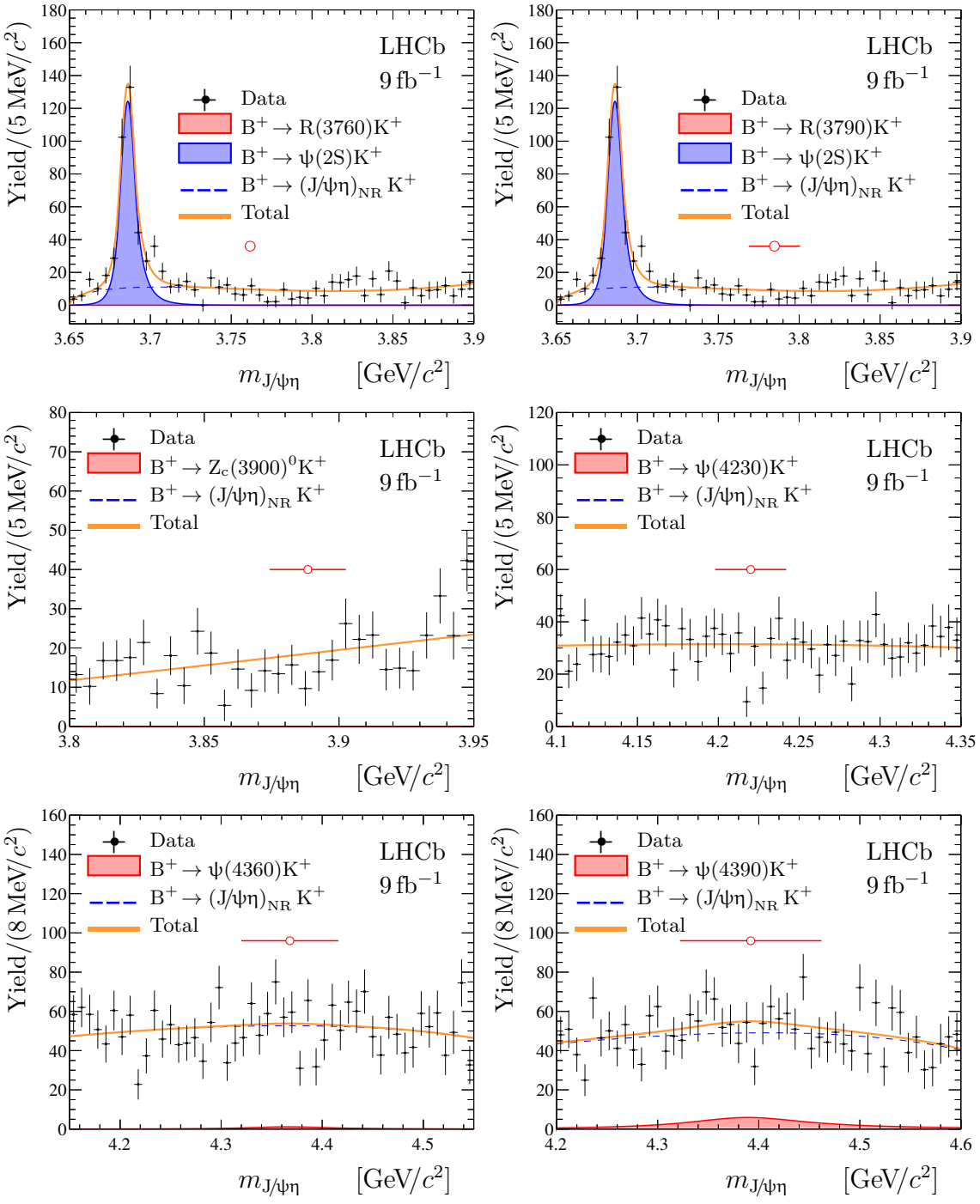

Figure 4. Background-subtracted J/ψη mass distribution from $B^+ \to J/\psi\eta K^+$ decays in the vicinity of the charmonum-like (top row) R(3760), R(3790), (middle row) $Z(3900)^0$, ψ(4230), (bottom row) ψ(4360) and ψ(4390) states. The results of the fits, described in the text, are overlaid. The red open point with horizontal error bars indicates the mass and width of the resonance assumed in the fits.

JHEP04(2022)046

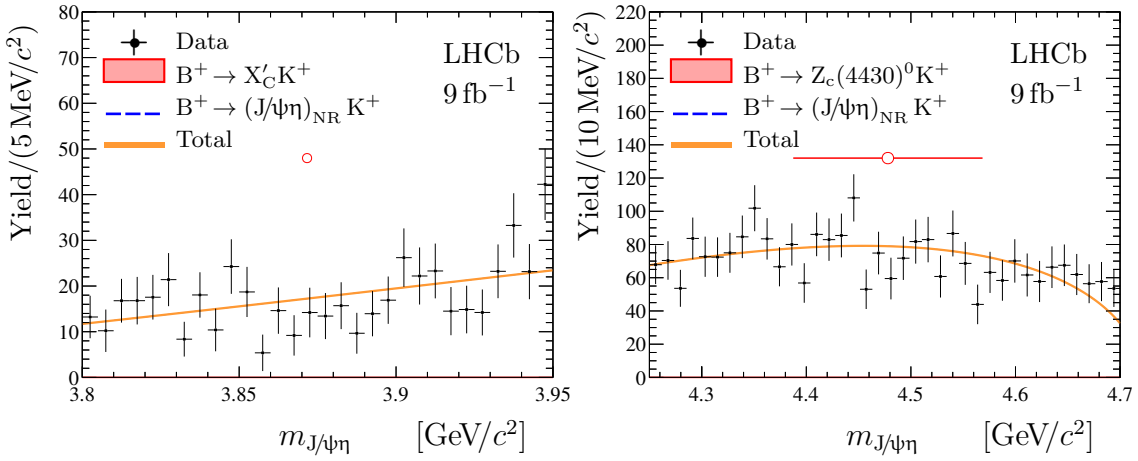

Figure 5. Background-subtracted J/ψη mass distribution from $B^+ \to J/\psi\eta K^+$ decays in the vicinity of the hypothetical (left) X'_C and (right) $Z_c(4430)^0$ states. The results of the fits, described in the text, are overlaid. The red open point with horizontal error bars indicates the mass and width of the resonance used in the fits.

Source	Uncertainty [%]
Simulation sample size	1.0–4.0
B^+ meson kinematics	0.1
Kaon identification	1.0
Tracking efficiency correction	0.02–0.15
Photon efficiency corrections	0.0–0.9
Trigger	1.1
Data-simulation agreement	4.0
Sum in quadrature	4.7–6.6

Table 1. Relative systematic uncertainties for the efficiency ratio R_ε. When an uncertainty is found to be dependent on the J/ψη mass, the corresponding range is shown. The total uncertainty is obtained as the quadratic sum of the individual contributions.

acceptance, and the trigger efficiency for decays passing the selection criteria. All efficiencies are calculated using simulation, as described in section 2. The finite size of the simulation samples contributes to the uncertainty on the $R_\varepsilon(m_X)$ ratio. Since signal and normalisation decays share the same final state, many systematic uncertainties cancel in the ratio R_ε. The remaining nonnegligible uncertainties are listed in table 1.

A large class of systematic uncertainties is associated to the corrections applied to the simulation. The finite size of the $B^+ \to J/\psi K^+$ signal sample used for correction of the simulated p_T and y spectra of B^+ mesons, induces a corresponding uncertainty. In turn, the variation within their uncertainties induces small changes in the ratio R_ε. The corresponding spread of these changes amounts to 0.1% and is taken as systematic uncertainty.

JHEP04(2022)046

The kaon identification variable used for the MLP estimator is drawn from calibration data samples accounting for the dependence on particle kinematics and track multiplicity. Systematic uncertainties in this procedure arise from the limited statistics of both the simulation and calibration samples, and the modelling of the identification variable. The limitations due to both simulation and calibration sample size are evaluated by bootstrapping to create multiple samples, and repeating the procedure for each sample. The impact of potential mismodelling of the kaon identification variable is evaluated by describing the corresponding distributions using density estimates with different kernel widths [92]. For each of these cases, alternative efficiency maps are produced to determine the associated uncertainties. A systematic uncertainty of 1% is assigned from the observed differences with alternative efficiency maps.

There are residual differences in the reconstruction efficiency of charged-particle tracks that do not cancel completely in the ratio R_ε due to the slightly different kinematic distributions of the final-state particles. The track-finding efficiencies obtained from simulated samples are corrected using calibration channels [93]. The uncertainties related to the efficiency correction factors are propagated to the ratios of the total efficiencies using pseudoexperiments and are found to be less than 0.15% for the considered values of the m_{X} parameter. Differences between data and simulation of photon reconstruction efficiencies are studied using a large sample of $\mathrm{B}^+ \to \mathrm{J/\psi}\,(\mathrm{K}^{*+} \to \mathrm{K}^+\,(\pi^0 \to \gamma\gamma))$ decays [94, 95, 110]. The uncertainties related to the photon efficiency correction factors are propagated to the ratios of the total efficiencies using pseudoexperiments and are found to be less than 0.9% for the considered values of the m_{X} parameter.

A systematic uncertainty related to the knowledge of the trigger efficiencies has been previously studied using large samples of $\mathrm{B}^+ \to (\mathrm{J/\psi} \to \mu^+\mu^-)\,\mathrm{K}^+$ and $\mathrm{B}^+ \to (\psi(2\mathrm{S}) \to \mu^+\mu^-)\,\mathrm{K}^+$ decays by comparing the ratios of the trigger efficiencies in data and simulation [111]. Based on this comparison, a relative uncertainty of 1.1% is assigned.

Another possible source of uncertainty is the potential disagreement between data and simulation in the estimation of efficiencies due to effects not considered above. This is studied by varying the selection criteria in ranges that lead to changes in the measured signal yields as large as ±20%. For this study, the $\mathrm{B}^+ \to (\psi(2\mathrm{S}) \to \mathrm{J/\psi\eta})\,\mathrm{K}^+$ data sample is used. The resulting difference in data-simulation efficiency ratio does not exceed 4.0%, which is conservatively taken as systematic uncertainty.

The systematic uncertainties discussed above affect the ratio of the total efficiencies R_ε, and are accounted for in the fits using Gaussian constraints. A different class of systematic uncertainties directly affects the fit itself, namely uncertainties associated with the fit models used to describe the $\mathrm{J/\psi\eta}$ and $\mathrm{J/\psi\eta K}^+$ mass spectra. The systematic uncertainty is accounted for by using fits with alternative models. The alternative resolution models for the $\mathcal{C}_{\psi(2\mathrm{S})}$ and $\mathcal{C}_{\mathrm{X}}$ components include a generalised Student's t-distribution [112] and a sum of two modified Gaussian functions with a power-law tail on each side of the distribution. For wide charmonia and charmonium-like resonances a P-wave relativistic Breit-Wigner function is also tested instead of the S-wave profile. The tail parameters of the $\mathcal{F}_{\mathcal{S}}$ resolution functions are varied within their uncertainties, as determined from the simulation. For the C_{NR} component, the degree of the polynomial function is varied

JHEP04(2022)046

between zero and two. For the signal component of the fit to the $J/\psi\eta K^+$ mass spectrum, the list of alternative models consists of a bifurcated generalised Student's t-distribution [112], an Apollonius function [113], and a sum of two modified Gaussian functions with a power-law tail on each side of the distribution. For the background component, the second-degree positive-definite polynomial function, and the product of an exponential function and a second-degree positive-definite polynomial function, are tested as alternative models. For each alternative model a fit to the $J/\psi\eta$ mass spectrum is performed and the upper limit (UL) on the F_X or B_X value is determined and conservatively the largest value of the upper limit is taken to account for the systematic uncertainty. For the $B^+ \to (\psi_2(3823) \to J/\psi\eta)\, K^+$ and $B^+ \to (\psi(4040) \to J/\psi\eta)\, K^+$ signals, the maximal deviation relative to the baseline fit is taken as uncertainty and added in quadrature to the uncertainty obtained from the fit. For the $\psi_2(3823)$ state, only 90 (95)% confidence level (CL) upper limits on the natural width of 5.2 (6.6) MeV are known [30]. For this case fits with the natural width varied between 0.2 and 6.6 MeV are performed and the maximal deviation with respect to the default fit, where 1 MeV is assumed, is taken as the corresponding systematic uncertainty.

6 Results and summary

The upper limits at 90% CL on the ratio of branching fractions $F_X(m_X)$ for $B^+ \to (X \to J/\psi\eta)\, K^+$ decays via a narrow intermediate X state are set for masses of the hypothetical X particle between 3.7 and 4.7 GeV/c^2. The upper limits, shown in figure 6, are set with the CL_s method [114] in which the p-values are calculated based on the asymptotic properties of the profile likelihood ratio [115]. The corresponding upper limits on the product of branching fractions, B_X, are calculated in a similar way and shown in figure 7. The local statistical significance for the mass values with the weakest upper limits, e.g. $m_X = 3.952$, 4.352 or 4.442 GeV/c^2, is estimated using Wilks' theorem [116] and is found to be less than three standard deviations.

Signals with a statistical significance exceeding three standard deviations are seen only for the $B^+ \to (\psi_2(3823) \to J/\psi\eta)\, K^+$ and $B^+ \to (\psi(4040) \to J/\psi\eta)\, K^+$ decays. The fit to the $J/\psi\eta$ mass distribution in the $\psi(4040)$ region suggests potential contributions from other resonances or sizeable interference effects, in particular with a possible $\psi(4160)$ contribution. Accounting for systematic uncertainties the significance is found to be 3.4 and 4.7 standard deviations for decays mediated by the $\psi_2(3823)$ and $\psi(4040)$ states, respectively.[2] The ratios of branching fractions are found to be

$$F_{\psi_2(3823)} = \left(5.95\, {}^{+3.38}_{-2.55}\right) \times 10^{-2}\,,$$
$$F_{\psi(4040)} = (40.6 \pm 11.2) \times 10^{-2}\,.$$

The asymmetric uncertainty in $F_{\psi_2(3823)}$ arises from varying the $\psi_2(3823)$ natural width between 0.2 and 6.6 MeV. The corresponding products of branching fractions are

$$B_{\psi_2(3823)} = \left(1.25\, {}^{+0.71}_{-0.53} \pm 0.04\right) \times 10^{-6}\,,$$
$$B_{\psi(4040)} = (8.53 \pm 2.35 \pm 0.30) \times 10^{-6}\,,$$

[2]For the wide $\psi(4040)$ state, the large reduction of the signal significance is due to the systematic uncertainty associated with the background parameterisation.

JHEP04(2022)046

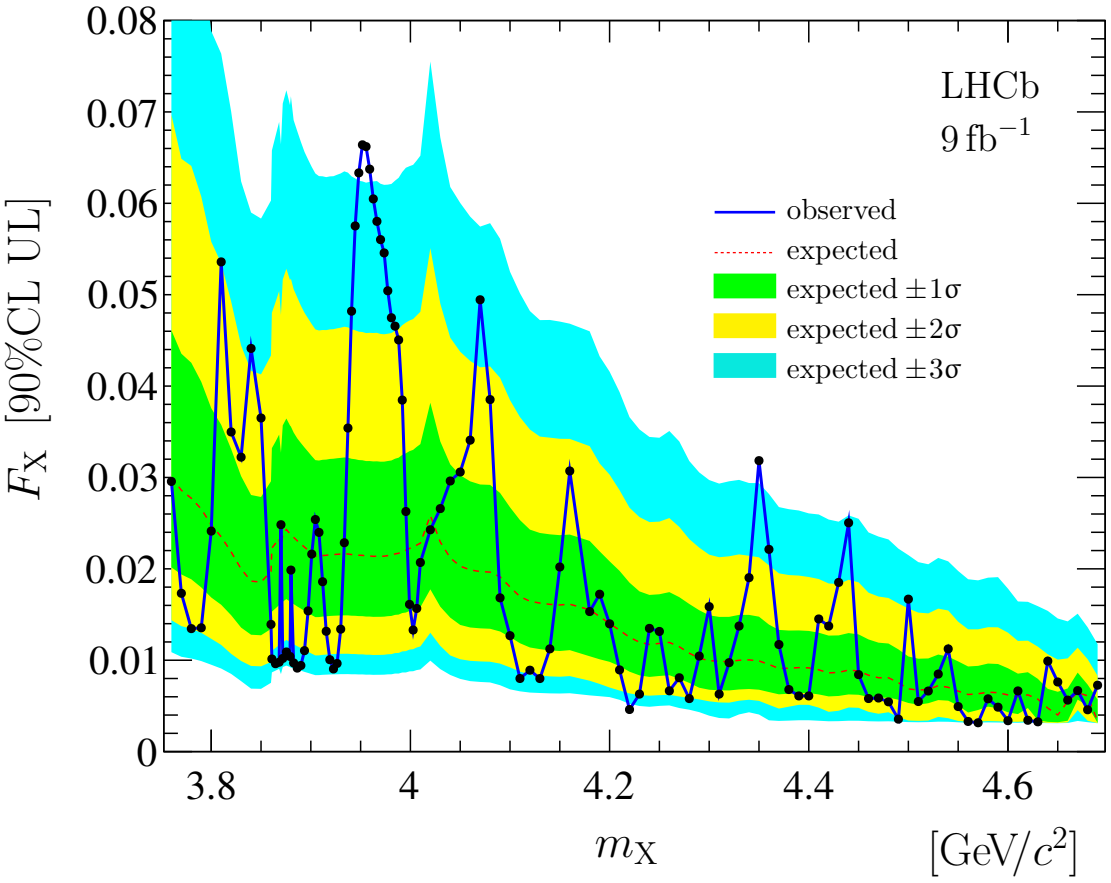

Figure 6. Upper limit (90% CL) on the ratio of branching fractions F_X as a function of the mass of the hypothetical narrow X state. The median expected upper limit together with the expected CL bands corresponding to 1, 2 and 3 standard deviations are also shown.

where the second uncertainty is due to the imprecise knowledge of the $B^+ \to \psi(2S)K^+$ and $\psi(2S) \to J/\psi\eta$ branching fractions [34]. For decays with other intermediate states no signals are seen and the corresponding upper limits are listed in table 2.

Using the value of $\mathcal{B}(B^+ \to \psi_2(3823)K^+) \times \mathcal{B}(\psi_2(3823) \to J/\psi\pi^+\pi^-)$ from ref. [30], the ratio of branching fractions for the $\psi_2(3823) \to J/\psi\eta$ and $\psi_2(3823) \to J/\psi\pi^+\pi^-$ decays is calculated to be

$$\frac{\mathcal{B}(\psi_2(3823) \to J/\psi\eta)}{\mathcal{B}(\psi_2(3823) \to J/\psi\pi^+\pi^-)} = 4.4\,^{+2.5}_{-1.9} \pm 0.9\,,$$

where the last uncertainty accounts for the precision on external branching fractions [30, 34]. Such a large partial width of the $\psi_2(3823) \to J/\psi\eta$ decay calls for a significant reevaluation of the $\psi_2(3823)$ branching fraction estimates of ref. [117]. This ratio is significantly larger than the value of $(9.72 \pm 0.14) \times 10^{-2}$ obtained for decays of the $\psi(2S)$ state. However, this might not be surprising as for higher charmonium excitations the charmonium-to-charmonium transitions with the emission of an η meson are not suppressed, e.g. for the $\psi(4040)$ state the corresponding ratio of transitions involving η and $\pi^+\pi^-$ exceeds unity [34].

JHEP04(2022)046

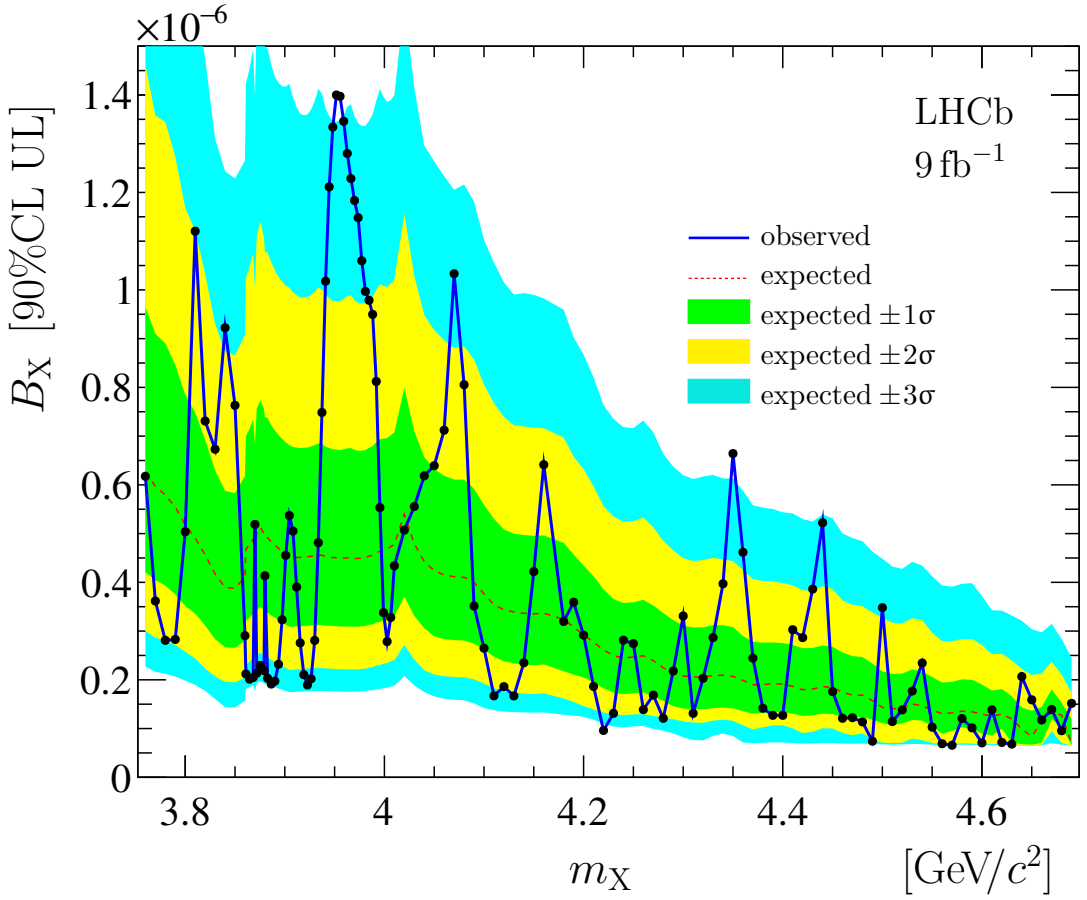

Figure 7. Upper limit (90% CL) on the product of branching fractions B_X as a function of the mass of the hypothetical narrow X state. The median expected upper limit together with the expected CL bands corresponding to 1, 2 and 3 standard deviations are also shown.

Using the previously measured value of the $\psi(4040) \to J/\psi\eta$ branching fraction from refs. [34, 118], the $B^+ \to \psi(4040)K^+$ branching fraction is calculated to be

$$\mathcal{B}(B^+ \to \psi(4040)K^+) = (1.64 \pm 0.45 \pm 0.23) \times 10^{-3}\,,$$

where the last uncertainty accounts for the $B^+ \to \psi(2S)K^+$, $\psi(2S) \to J/\psi\eta$ and $\psi(4040) \to J/\psi\eta$ branching fraction uncertainties. This disagrees with the upper limit of 1.3×10^{-4} at 90% CL from ref. [119], which used the $\psi(4040) \to \mu^+\mu^-$ decay mode and relied on the $\psi(4040) \to \mu^+\mu^-$ branching fraction from ref. [120] to obtain a B^+ decay limit. This disagreement motivates a more detailed study of this system, such as a full amplitude analysis. In ref. [121] it was demonstrated that the $B^+ \to (\psi(4040) \to D^+D^-)\,K^+$ and $B^+ \to (\psi(4160) \to D^+D^-)\,K^+$ decays have comparable rates. In this paper a significant suppression of the $\psi(4160) \to J/\psi\eta$ transitions relative to such transitions for the $\psi(4040)$ state is found. The opposite pattern was found in the analysis of $B^+ \to K^+\mu^+\mu^-$ decays [119], where a large contribution from decays via the intermediate $\psi(4160)$ state is observed, while no decays with the intermediate $\psi(4040)$ state are seen.

JHEP04(2022)046

	Upper limit at 90% CL	
	$F_{\rm X}$ $[10^{-2}]$	$B_{\rm X}$ $[10^{-7}]$
$\psi(3770)$	2.2	4.6
$\psi_3(3842)$	2.9	6.1
$\psi(4160)$	4.2	8.7
$\psi(4415)$	4.6	9.6
R(3760)	2.0	4.1
R(3790)	3.2	6.7
$\mathrm{Z_c}(3900)^0$	2.1	4.3
$\psi(4230)$	1.9	3.9
$\psi(4360)$	6.0	12.4
$\psi(4390)$	11.6	24.1
$\mathrm{Z_c}(4430)^0$	6.1	12.7
$\mathrm{X'_C}$	1.9	3.9

Table 2. Upper limits at 90% CL for the ratio of branching fractions $F_{\rm X}$ and product of branching fractions $B_{\rm X}$ for different conventional charmonia, charmonium-like and hypothetical states.

No signals are found for the $\mathrm{B^+ \to J/\psi \eta K^+}$ decay via conventional charmonium states $\psi(3770)$, $\psi_3(3842)$, $\psi(4160)$, $\psi(4415)$; charmonium-like states R(3760), R(3790), $\mathrm{Z_c}(3900)^0$, $\psi(4230)$, $\psi(4360)$ and $\psi(4390)$; the hypothetical neutral partner of the charged $\mathrm{Z_c}(4430)^+$ state; and for the hypothetical C-odd partner of the $\chi_{c1}(3872)$ state, $\mathrm{X'_C}$. In particular, for the latter upper limits at 90% CL are found to be

$$F_{\mathrm{X'_C}} < 1.9 \times 10^{-2}\,,$$
$$B_{\mathrm{X'_C}} < 3.9 \times 10^{-7}\,,$$

significantly improving results previously obtained by the BaBar and Belle collaborations [65, 66].

In conclusion, a search for charmonium and charmonium-like exotic states contributing to the $\mathrm{J/\psi\eta}$ mass spectrum from $\mathrm{B^+ \to J/\psi \eta K^+}$ decays is performed, using a data sample corresponding to an integrated luminosity of $9\,\mathrm{fb}^{-1}$ collected with the LHCb detector at 7, 8 and 13 TeV centre-of-mass energies in proton-proton collisions. The $\mathrm{B^+ \to (\psi(2S) \to J/\psi \eta)\, K^+}$ decay mode is used a normalisation channel. While no narrow resonances are seen, evidence is found for the $\mathrm{B^+ \to (\psi_2(3823) \to J/\psi \eta)\, K^+}$ and $\mathrm{B^+ \to (\psi(4040) \to J/\psi \eta)\, K^+}$ decays, and the corresponding branching fractions and their ratios relative to the normalisation decay mode are measured.

JHEP04(2022)046

Acknowledgments

We express our gratitude to our colleagues in the CERN accelerator departments for the excellent performance of the LHC. We thank the technical and administrative staff at the LHCb institutes. We acknowledge support from CERN and from the national agencies: CAPES, CNPq, FAPERJ and FINEP (Brazil); MOST and NSFC (China); CNRS/IN2P3 (France); BMBF, DFG and MPG (Germany); INFN (Italy); NWO (Netherlands); MNiSW and NCN (Poland); MEN/IFA (Romania); MSHE (Russia); MICINN (Spain); SNSF and SER (Switzerland); NASU (Ukraine); STFC (United Kingdom); DOE NP and NSF (U.S.A.). We acknowledge the computing resources that are provided by CERN, IN2P3 (France), KIT and DESY (Germany), INFN (Italy), SURF (Netherlands), PIC (Spain), GridPP (United Kingdom), RRCKI and Yandex LLC (Russia), CSCS (Switzerland), IFIN-HH (Romania), CBPF (Brazil), PL-GRID (Poland) and NERSC (U.S.A.). We are indebted to the communities behind the multiple open-source software packages on which we depend. Individual groups or members have received support from ARC and ARDC (Australia); AvH Foundation (Germany); EPLANET, Marie Skłodowska-Curie Actions and ERC (European Union); A*MIDEX, ANR, Labex P2IO and OCEVU, and Région Auvergne-Rhône-Alpes (France); Key Research Program of Frontier Sciences of CAS, CAS PIFI, CAS CCEPP, Fundamental Research Funds for the Central Universities, and Sci. & Tech. Program of Guangzhou (China); RFBR, RSF and Yandex LLC (Russia); GVA, XuntaGal and GENCAT (Spain); the Leverhulme Trust, the Royal Society and UKRI (United Kingdom).

References

[1] Belle collaboration, *Observation of a narrow charmonium-like state in exclusive* $B^{\pm} \to K^{\pm}\pi^{+}\pi^{-}J/\psi$ *decays*, *Phys. Rev. Lett.* **91** (2003) 262001 [hep-ex/0309032] [INSPIRE].

[2] CDF collaboration, *Observation of the narrow state* $X(3872) \to J/\psi\pi^{+}\pi^{-}$ *in* $\overline{p}p$ *collisions at* $\sqrt{s} = 1.96$ *TeV*, *Phys. Rev. Lett.* **93** (2004) 072001 [hep-ex/0312021] [INSPIRE].

[3] D0 collaboration, *Observation and properties of the* $X(3872)$ *decaying to* $J/\psi\pi^{+}\pi^{-}$ *in* $p\overline{p}$ *collisions at* $\sqrt{s} = 1.96$ *TeV*, *Phys. Rev. Lett.* **93** (2004) 162002 [hep-ex/0405004] [INSPIRE].

[4] BaBar collaboration, *Study of the* $B^{-} \to J/\psi K^{-}\pi^{+}\pi^{-}$ *decay and measurement of the* $B^{-} \to J/\psi K^{-}\pi^{+}\pi^{-}$ *branching fraction*, *Phys. Rev. D* **71** (2005) 071103 [hep-ex/0406022] [INSPIRE].

[5] CDF collaboration, *Measurement of the dipion mass spectrum in* $X(3872) \to J/\psi\pi^{+}\pi^{-}$ *decays*, *Phys. Rev. Lett.* **96** (2006) 102002 [hep-ex/0512074] [INSPIRE].

[6] BaBar collaboration, *Study of the* $X(3872)$ *and* $Y(4260)$ *in* $B^{0} \to J/\psi\pi^{+}\pi^{-}K^{0}$ *and* $B^{-} \to J/\psi\pi^{+}\pi^{-}K^{-}$ *decays*, *Phys. Rev. D* **73** (2006) 011101 [hep-ex/0507090] [INSPIRE].

[7] BaBar collaboration, *Search for* $B^{+} \to X(3872)K^{+}$, $X(3872) \to J/\psi\gamma$, *Phys. Rev. D* **74** (2006) 071101 [hep-ex/0607050] [INSPIRE].

JHEP04(2022)046

[8] CDF collaboration, *Analysis of the quantum numbers* J^{PC} *of the* X(3872) *particle*, *Phys. Rev. Lett.* **98** (2007) 132002 [hep-ex/0612053] [INSPIRE].

[9] BABAR collaboration, *Search for prompt production of* χ_c *and* X(3872) *in* e^+e^- *annihilations*, *Phys. Rev. D* **76** (2007) 071102 [arXiv:0707.1633] [INSPIRE].

[10] BABAR collaboration, *Study of* $B \to X(3872)K$, *with* $X(3872) \to J/\psi\pi^+\pi^-$, *Phys. Rev. D* **77** (2008) 111101 [arXiv:0803.2838] [INSPIRE].

[11] CDF collaboration, *Precision measurement of the* X(3872) *mass in* $J/\psi\pi^+\pi^-$ *decays*, *Phys. Rev. Lett.* **103** (2009) 152001 [arXiv:0906.5218] [INSPIRE].

[12] BABAR collaboration, *Evidence for* $X(3872) \to \psi(2S)\gamma$ *in* $B^\pm \to X(3872)K^\pm$ *decays, and a study of* $B \to c\bar{c}\gamma K$, *Phys. Rev. Lett.* **102** (2009) 132001 [arXiv:0809.0042] [INSPIRE].

[13] BELLE collaboration, *Study of the* $B \to X(3872)(\to D^{*0}\overline{D}^0)K$ *decay*, *Phys. Rev. D* **81** (2010) 031103 [arXiv:0810.0358] [INSPIRE].

[14] BABAR collaboration, *Evidence for the decay* $X(3872) \to J/\psi\omega$, *Phys. Rev. D* **82** (2010) 011101 [arXiv:1005.5190] [INSPIRE].

[15] BELLE collaboration, *Bounds on the width, mass difference and other properties of* $X(3872) \to \pi^+\pi^- J/\psi$ *decays*, *Phys. Rev. D* **84** (2011) 052004 [arXiv:1107.0163] [INSPIRE].

[16] BELLE collaboration, *Observation of* $X(3872) \to J/\psi\gamma$ *and search for* $X(3872) \to \psi'\gamma$ *in* B *decays*, *Phys. Rev. Lett.* **107** (2011) 091803 [arXiv:1105.0177] [INSPIRE].

[17] LHCb collaboration, *Observation of* X(3872) *production in* pp *collisions at* $\sqrt{s} = 7$ *TeV*, *Eur. Phys. J. C* **72** (2012) 1972 [arXiv:1112.5310] [INSPIRE].

[18] LHCb collaboration, *Determination of the* X(3872) *meson quantum numbers*, *Phys. Rev. Lett.* **110** (2013) 222001 [arXiv:1302.6269] [INSPIRE].

[19] CMS collaboration, *Measurement of the* X(3872) *production cross section via decays to* $J/\psi\pi^+\pi^-$ *in* pp *collisions at* $\sqrt{s} = 7$ *TeV*, *JHEP* **04** (2013) 154 [arXiv:1302.3968] [INSPIRE].

[20] BESIII collaboration, *Observation of* $e^+e^- \to \gamma X(3872)$ *at BESIII*, *Phys. Rev. Lett.* **112** (2014) 092001 [arXiv:1310.4101] [INSPIRE].

[21] LHCb collaboration, *Evidence for the decay* $X(3872) \to \psi(2S)\gamma$, *Nucl. Phys. B* **886** (2014) 665 [arXiv:1404.0275] [INSPIRE].

[22] BELLE collaboration, *Observation of* X(3872) *in* $B \to X(3872)K\pi$ *decays*, *Phys. Rev. D* **91** (2015) 051101 [arXiv:1501.06867] [INSPIRE].

[23] LHCb collaboration, *Quantum numbers of the* X(3872) *state and orbital angular momentum in its* $\rho^0 J/\psi$ *decays*, *Phys. Rev. D* **92** (2015) 011102 [arXiv:1504.06339] [INSPIRE].

[24] ATLAS collaboration, *Measurements of* $\psi(2S)$ *and* $X(3872) \to J/\psi\pi^+\pi^-$ *production in* pp *collisions at* $\sqrt{s} = 8$ *TeV with the ATLAS detector*, *JHEP* **01** (2017) 117 [arXiv:1610.09303] [INSPIRE].

[25] LHCb collaboration, *Observation of* $\eta_c(2S) \to p\bar{p}$ *and search for* $X(3872) \to p\bar{p}$ *decays*, *Phys. Lett. B* **769** (2017) 305 [arXiv:1607.06446] [INSPIRE].

[26] LHCb collaboration, *Observation of the* $\Lambda_b^0 \to \chi_{c1}(3872)pK^-$ *decay*, *JHEP* **09** (2019) 028 [arXiv:1907.00954] [INSPIRE].

[27] BELLE collaboration, *Search for* $B^0 \to X(3872)\gamma$, *Phys. Rev. D* **100** (2019) 012002 [arXiv:1905.11718] [INSPIRE].

JHEP04(2022)046

[28] Belle collaboration, *Search for* X(3872) *and* X(3915) *decay into* $\chi_{c1}\pi^0$ *in* B *decays at Belle*, *Phys. Rev. D* **99** (2019) 111101 [arXiv:1904.07015] [INSPIRE].

[29] LHCb collaboration, *Study of the line shape of the* $\chi_{c1}(3872)$ *state*, *Phys. Rev. D* **102** (2020) 092005 [arXiv:2005.13419] [INSPIRE].

[30] LHCb collaboration, *Study of the* $\psi_2(3823)$ *and* $\chi_{c1}(3872)$ *states in* $B^+ \to (J/\psi\pi^+\pi^-)\,K^+$ *decays*, *JHEP* **08** (2020) 123 [arXiv:2005.13422] [INSPIRE].

[31] LHCb collaboration, *Modification of* $\chi_{c1}(3872)$ *and* $\psi(2S)$ *production in pp collisions at* $\sqrt{s} = 8$ *TeV*, *Phys. Rev. Lett.* **126** (2021) 092001 [arXiv:2009.06619] [INSPIRE].

[32] CMS collaboration, *Observation of the* $B_s^0 \to X(3872)\phi$ *decay*, *Phys. Rev. Lett.* **125** (2020) 152001 [arXiv:2005.04764] [INSPIRE].

[33] LHCb collaboration, *Study of* $B_s^0 \to J/\psi\pi^+\pi^-K^+K^-$ *decays*, *JHEP* **02** (2021) 024 [*Erratum ibid.* **04** (2021) 170] [arXiv:2011.01867] [INSPIRE].

[34] Particle Data Group collaboration, *Review of particle physics*, *PTEP* **2020** (2020) 083C01 [INSPIRE] and 2021 update.

[35] N. Brambilla et al., *The* XYZ *states: experimental and theoretical status and perspectives*, *Phys. Rept.* **873** (2020) 1 [arXiv:1907.07583] [INSPIRE].

[36] E.S. Swanson, *The new heavy mesons: A status report*, *Phys. Rept.* **429** (2006) 243 [hep-ph/0601110] [INSPIRE].

[37] H.-X. Chen, W. Chen, X. Liu and S.-L. Zhu, *The hidden-charm pentaquark and tetraquark states*, *Phys. Rept.* **639** (2016) 1 [arXiv:1601.02092] [INSPIRE].

[38] A. Esposito, A. Pilloni and A.D. Polosa, *Multiquark resonances*, *Phys. Rept.* **668** (2017) 1 [arXiv:1611.07920] [INSPIRE].

[39] A. Ali, J.S. Lange and S. Stone, *Exotics: Heavy pentaquarks and tetraquarks*, *Prog. Part. Nucl. Phys.* **97** (2017) 123 [arXiv:1706.00610] [INSPIRE].

[40] A. Hosaka, T. Iijima, K. Miyabayashi, Y. Sakai and S. Yasui, *Exotic hadrons with heavy flavors:* X*,* Y*,* Z*, and related states*, *PTEP* **2016** (2016) 062C01 [arXiv:1603.09229] [INSPIRE].

[41] R.F. Lebed, R.E. Mitchell and E.S. Swanson, *Heavy-quark QCD exotica*, *Prog. Part. Nucl. Phys.* **93** (2017) 143 [arXiv:1610.04528] [INSPIRE].

[42] F.-K. Guo, C. Hanhart, U.-G. Meißner, Q. Wang, Q. Zhao and B.-S. Zou, *Hadronic molecules*, *Rev. Mod. Phys.* **90** (2018) 015004 [arXiv:1705.00141] [INSPIRE].

[43] S.L. Olsen, T. Skwarnicki and D. Zieminska, *Nonstandard heavy mesons and baryons: Experimental evidence*, *Rev. Mod. Phys.* **90** (2018) 015003 [arXiv:1708.04012] [INSPIRE].

[44] A. Ali, L. Maiani and A.D. Polosa, *Multiquark hadrons*, Cambridge University Press, Cambridge, U.K. (2019) [DOI] [INSPIRE].

[45] E.S. Swanson, *Molecular interpretation of the* X(3872), in *32nd International Conference on High Energy Physics*, pp. 1037–1039 (2004) [DOI] [hep-ph/0410284] [INSPIRE].

[46] X. Liu, Z.-G. Luo, Y.-R. Liu and S.-L. Zhu, X(3872) *and other possible heavy molecular states*, *Eur. Phys. J. C* **61** (2009) 411 [arXiv:0808.0073] [INSPIRE].

[47] I.W. Lee, A. Faessler, T. Gutsche and V.E. Lyubovitskij, X(3872) *as a molecular* $D\overline{D}^*$ *state in a potential model*, *Phys. Rev. D* **80** (2009) 094005 [arXiv:0910.1009] [INSPIRE].

JHEP04(2022)046

[48] P.G. Ortega, J. Segovia, D.R. Entem and F. Fernandez, *The* X(3872) *an other possible* XYZ *molecular states*, *AIP Conf. Proc.* **1257** (2010) 331 [arXiv:1001.3948] [INSPIRE].

[49] M. Albaladejo et al., *Note on* X(3872) *production at hadron colliders and its molecular structure*, *Chin. Phys. C* **41** (2017) 121001 [arXiv:1709.09101] [INSPIRE].

[50] Y.S. Kalashnikova and A.V. Nefediev, X(3872) *in the molecular model*, *Phys. Usp.* **62** (2019) 568 [arXiv:1811.01324] [INSPIRE].

[51] F.-L. Wang, X.-D. Yang, R. Chen and X. Liu, *Finding new evidence to identify charmoniumlike molecules*, *Phys. Rev. D* **104** (2021) 094010 [arXiv:2103.04698] [INSPIRE].

[52] L. Maiani, F. Piccinini, A.D. Polosa and V. Riquer, *Diquark-antidiquarks with hidden or open charm and the nature of* X(3872), *Phys. Rev. D* **71** (2005) 014028 [hep-ph/0412098] [INSPIRE].

[53] L. Maiani, F. Piccinini, A.D. Polosa and V. Riquer, *The* Z(4430) *and a new paradigm for spin interactions in tetraquarks*, *Phys. Rev. D* **89** (2014) 114010 [arXiv:1405.1551] [INSPIRE].

[54] L. Maiani, A.D. Polosa and V. Riquer, *A theory of* X *and* Z *multiquark resonances*, *Phys. Lett. B* **778** (2018) 247 [arXiv:1712.05296] [INSPIRE].

[55] B.A. Li, *Is* X(3872) *a possible candidate as a hybrid meson?*, *Phys. Lett. B* **605** (2005) 306 [hep-ph/0410264] [INSPIRE].

[56] M.T. AlFiky, *Molecular description of* X(3872) *in effective field theory*, *J. Phys. Conf. Ser.* **69** (2007) 012005 [INSPIRE].

[57] S. Dubynskiy and M.B. Voloshin, *Hadro-charmonium*, *Phys. Lett. B* **666** (2008) 344 [arXiv:0803.2224] [INSPIRE].

[58] N.N. Achasov and E.V. Rogozina, *Towards the nature of* X(3872) *resonance*, *J. Univ. Sci. Tech. China* **46** (2016) 574 [arXiv:1510.07251] [INSPIRE].

[59] N.N. Achasov and E.V. Rogozina, X(3872), $I^G(J^{PC}) = 0^+(1^{++})$, *as the* $\chi_{c1}(2P)$ *charmonium*, *Mod. Phys. Lett. A* **30** (2015) 1550181 [arXiv:1501.03583] [INSPIRE].

[60] F.K. Guo, C. Hidalgo-Duque, J. Nieves and M.P. Valderrama, *Heavy quark symmetries: Molecular partners of the* X(3872) *and* $Z_b(10610)/Z_b'(10650)$, *Int. J. Mod. Phys. Conf. Ser.* **26** (2014) 1460073 [arXiv:1309.3865] [INSPIRE].

[61] V. Baru, E. Epelbaum, A.A. Filin, C. Hanhart and A.V. Nefediev, *Heavy-quark spin symmetry partners of the* X(3872) *molecule*, *JPS Conf. Proc.* **13** (2017) 020023 [INSPIRE].

[62] V. Baru, E. Epelbaum, A.A. Filin, C. Hanhart and A.V. Nefediev, *Molecular partners of the* X(3872) *from heavy-quark spin symmetry: A fresh look*, *EPJ Web Conf.* **137** (2017) 06002 [INSPIRE].

[63] H. Mutuk, Y. Saraç, H. Gümüs and A. Ozpineci, X(3872) *and its heavy quark spin symmetry partners in QCD sum rules*, *Eur. Phys. J. C* **78** (2018) 904 [arXiv:1807.04091] [INSPIRE].

[64] M.-Z. Liu, T.-W. Wu, M. Pavon Valderrama, J.-J. Xie and L.-S. Geng, *Heavy-quark spin and flavor symmetry partners of the* X(3872) *revisited: What can we learn from the one boson exchange model?*, *Phys. Rev. D* **99** (2019) 094018 [arXiv:1902.03044] [INSPIRE].

[65] BABAR collaboration, *Observation of the decay* $B \to J/\psi\eta K$ *and search for* $X(3872) \to J/\psi\eta$, *Phys. Rev. Lett.* **93** (2004) 041801 [hep-ex/0402025] [INSPIRE].

JHEP04(2022)046

[66] Belle collaboration, *Measurement of branching fractions for* $B \to J/\psi\eta K$ *decays and search for a narrow resonance in the* $J/\psi\eta$ *final state*, *PTEP* **2014** (2014) 043C01 [arXiv:1310.2704] [INSPIRE].

[67] LHCb collaboration, *Near-threshold* $D\overline{D}$ *spectroscopy and observation of a new charmonium state*, *JHEP* **07** (2019) 035 [arXiv:1903.12240] [INSPIRE].

[68] BESIII collaboration, *Observation of di-structures in* $e^+e^- \to J/\psi X$ *at center-of-mass energies around 3.773 GeV*, *Phys. Rev. Lett.* **127** (2021) 082002 [arXiv:2012.04186] [INSPIRE].

[69] BESIII collaboration, *Observation of* $Z_c(3900)$ *in* $e^+e^- \to \pi^0\pi^0 J/\psi$, *Phys. Rev. Lett.* **115** (2015) 112003 [arXiv:1506.06018] [INSPIRE].

[70] T. Xiao, S. Dobbs, A. Tomaradze and K.K. Seth, *Observation of the charged hadron* $Z_c(3900)^\pm$ *and evidence for the neutral* $Z_c(3900)^0$ *in* $e^+e^- \to \pi\pi J/\psi$ *at* $\sqrt{s} = 4170$ *MeV*, *Phys. Lett. B* **727** (2013) 366 [arXiv:1304.3036] [INSPIRE].

[71] BESIII collaboration, *Precise measurement of the* $e^+e^- \to \pi^+\pi^- J/\psi$ *cross section at center-of-mass energies from* 3.77 *to* 4.60 *GeV*, *Phys. Rev. Lett.* **118** (2017) 092001 [arXiv:1611.01317] [INSPIRE].

[72] BaBar collaboration, *Evidence of a broad structure at an invariant mass of* 4.32 GeV/c^2 *in the reaction* $e^+e^- \to \pi^+\pi^-\psi(2S)$ *measured at BaBar*, *Phys. Rev. Lett.* **98** (2007) 212001 [hep-ex/0610057] [INSPIRE].

[73] Belle collaboration, *Observation of two resonant structures in* $e^+e^- \to \pi^+\pi^-\psi(2S)$ *via initial state radiation at Belle*, *Phys. Rev. Lett.* **99** (2007) 142002 [arXiv:0707.3699] [INSPIRE].

[74] BaBar collaboration, *Study of the reaction* $e^+e^- \to \psi(2S)\pi^+\pi^-$ *via initial-state radiation at BaBar*, *Phys. Rev. D* **89** (2014) 111103 [arXiv:1211.6271] [INSPIRE].

[75] BESIII collaboration, *Evidence of two resonant structures in* $e^+e^- \to \pi^+\pi^- h_c$, *Phys. Rev. Lett.* **118** (2017) 092002 [arXiv:1610.07044] [INSPIRE].

[76] BESIII collaboration, *Observation of the* $Y(4220)$ *and* $Y(4360)$ *in the process* $e^+e^- \to \eta J/\psi$, *Phys. Rev. D* **102** (2020) 031101 [arXiv:2003.03705] [INSPIRE].

[77] Belle collaboration, *Observation of a resonance-like structure in the* $\pi^\pm\psi'$ *mass distribution in exclusive* $B \to K\pi^\pm\psi'$ *decays*, *Phys. Rev. Lett.* **100** (2008) 142001 [arXiv:0708.1790] [INSPIRE].

[78] Belle collaboration, *Experimental constraints on the spin and parity of the* $Z(4430)^+$, *Phys. Rev. D* **88** (2013) 074026 [arXiv:1306.4894] [INSPIRE].

[79] LHCb collaboration, *Observation of the resonant character of the* $Z(4430)^-$ *state*, *Phys. Rev. Lett.* **112** (2014) 222002 [arXiv:1404.1903] [INSPIRE].

[80] Belle collaboration, *Observation of a new charged charmoniumlike state in* $\overline{B}^0 \to J/\psi K^-\pi^+$ *decays*, *Phys. Rev. D* **90** (2014) 112009 [arXiv:1408.6457] [INSPIRE].

[81] LHCb collaboration, *Model-independent confirmation of the* $Z(4430)^-$ *state*, *Phys. Rev. D* **92** (2015) 112009 [arXiv:1510.01951] [INSPIRE].

[82] LHCb collaboration, *The LHCb detector at the LHC*, 2008 *JINST* **3** S08005 [INSPIRE].

[83] LHCb collaboration, *LHCb detector performance*, *Int. J. Mod. Phys. A* **30** (2015) 1530022 [arXiv:1412.6352] [INSPIRE].

JHEP04(2022)046

[84] C. Abellán Beteta et al., *Calibration and performance of the LHCb calorimeters in Run 1 and 2 at the LHC*, arXiv:2008.11556 [INSPIRE].

[85] T. Sjöstrand, S. Mrenna and P.Z. Skands, *A brief introduction to* PYTHIA 8.1, *Comput. Phys. Commun.* **178** (2008) 852 [arXiv:0710.3820] [INSPIRE].

[86] I. Belyaev et al., *Handling of the generation of primary events in Gauss, the LHCb simulation framework*, *J. Phys. Conf. Ser.* **331** (2011) 032047 [INSPIRE].

[87] D.J. Lange, *The* EVTGEN *particle decay simulation package*, *Nucl. Instrum. Meth. A* **462** (2001) 152 [INSPIRE].

[88] N. Davidson, T. Przedzinski and Z. Was, PHOTOS *interface in C++: Technical and physics documentation*, *Comput. Phys. Commun.* **199** (2016) 86 [arXiv:1011.0937] [INSPIRE].

[89] GEANT4 collaboration, GEANT4 *developments and applications*, *IEEE Trans. Nucl. Sci.* **53** (2006) 270 [INSPIRE].

[90] GEANT4 collaboration, GEANT4*: A simulation toolkit*, *Nucl. Instrum. Meth. A* **506** (2003) 250 [INSPIRE].

[91] M. Clemencic et al., *The LHCb simulation application,* GAUSS*: Design, evolution and experience*, *J. Phys. Conf. Ser.* **331** (2011) 032023 [INSPIRE].

[92] R. Aaij et al., *Selection and processing of calibration samples to measure the particle identification performance of the LHCb experiment in Run 2*, *EPJ Tech. Instrum.* **6** (2019) 1 [arXiv:1803.00824] [INSPIRE].

[93] LHCb collaboration, *Measurement of the track reconstruction efficiency at LHCb*, 2015 *JINST* **10** P02007 [arXiv:1408.1251] [INSPIRE].

[94] LHCb collaboration, *Evidence for the decay* $B^0 \to J/\psi\omega$ *and measurement of the relative branching fractions of* B_s^0 *meson decays to* $J/\psi\eta$ *and* $J/\psi\eta'$, *Nucl. Phys. B* **867** (2013) 547 [arXiv:1210.2631] [INSPIRE].

[95] LHCb collaboration, *Observations of* $B_s^0 \to \psi(2S)\eta$ *and* $B_{(s)}^0 \to \psi(2S)\pi^+\pi^-$ *decays*, *Nucl. Phys. B* **871** (2013) 403 [arXiv:1302.6354] [INSPIRE].

[96] LHCb collaboration, *Observation of* $B_s^0 \to \chi_{c1}\phi$ *decay and study of* $B^0 \to \chi_{c1,2}K^{*0}$ *decays*, *Nucl. Phys. B* **874** (2013) 663 [arXiv:1305.6511] [INSPIRE].

[97] LHCb collaboration, *Study of* η–η' *mixing from measurement of* $B_{(s)}^0 \to J/\psi\eta^{(\prime)}$ *decay rates*, *JHEP* **01** (2015) 024 [arXiv:1411.0943] [INSPIRE].

[98] LHCb collaboration, *Observation of the decay* $\Lambda_b^0 \to \chi_{c1}p\pi^-$, *JHEP* **05** (2021) 095 [arXiv:2103.04949] [INSPIRE].

[99] W.S. McCulloch and W. Pitts, *A logical calculus of the ideas immanent in nervous activity*, *Bull. Math. Biophys.* **5** (1943) 115.

[100] F. Rosenblatt, *The perceptron: A probabilistic model for information storage and organization in the brain*, *Psychol. Rev.* **65** (1958) 386.

[101] J.-H. Zhong, R.-S. Huang, S.-C. Lee, R.-S. Huang and S.-C. Lee, *A program for the Bayesian neural network in the* ROOT *framework*, *Comput. Phys. Commun.* **182** (2011) 2655 [arXiv:1103.2854] [INSPIRE].

[102] A. Powell et al., *Particle identification at LHCb*, *PoS* **ICHEP2010** (2010) 020 [INSPIRE].

JHEP04(2022)046

[103] H. Terrier and I. Belyaev, *Particle identification with LHCb calorimeters*, LHCb-2003-092, (2003).

[104] W.D. Hulsbergen, *Decay chain fitting with a Kalman filter*, *Nucl. Instrum. Meth. A* **552** (2005) 566 [physics/0503191] [INSPIRE].

[105] S. Geisser, *Predictive inference: An introduction*, Monographs on statistics and applied probability, Chapman & Hall, New York, U.S.A. (1993) [DOI].

[106] T. Skwarnicki, *A study of the radiative cascade transitions between the* Υ' *and* Υ *resonances*, Ph.D. Thesis, Institute of Nuclear Physics, Krakow (1986) [DESY-F31-86-02] [INSPIRE].

[107] LHCb collaboration, *Observation of* J/ψ*-pair production in* pp *collisions at* $\sqrt{s} = 7$ *TeV*, *Phys. Lett. B* **707** (2012) 52 [arXiv:1109.0963] [INSPIRE].

[108] M. Pivk and F.R. Le Diberder, *sPlot: A statistical tool to unfold data distributions*, *Nucl. Instrum. Meth. A* **555** (2005) 356 [physics/0402083] [INSPIRE].

[109] E. Byckling and K. Kajantie, *Particle kinematics*, John Wiley & Sons Inc., New York, U.S.A. (1973).

[110] E. Govorkova, *Study of* π^0/γ *efficiency using* B *meson decays in the LHCb experiment*, *Phys. Atom. Nucl.* **79** (2016) 1474 [arXiv:1505.02960] [INSPIRE].

[111] LHCb collaboration, *Measurement of relative branching fractions of* B *decays to* $\psi(2S)$ *and* J/ψ *mesons*, *Eur. Phys. J. C* **72** (2012) 2118 [arXiv:1205.0918] [INSPIRE].

[112] W.S. Gosset, *The probable error of a mean*, *Biometrika* **6** (1908) 1.

[113] D. Martínez Santos and F. Dupertuis, *Mass distributions marginalized over per-event errors*, *Nucl. Instrum. Meth. A* **764** (2014) 150 [arXiv:1312.5000] [INSPIRE].

[114] A.L. Read, *Presentation of search results: The* CL_s *technique*, *J. Phys. G* **28** (2002) 2693 [INSPIRE].

[115] G. Cowan, K. Cranmer, E. Gross and O. Vitells, *Asymptotic formulae for likelihood-based tests of new physics*, *Eur. Phys. J. C* **71** (2011) 1554 [*Erratum ibid.* **73** (2013) 2501] [arXiv:1007.1727] [INSPIRE].

[116] S.S. Wilks, *The Large-Sample Distribution of the Likelihood Ratio for Testing Composite Hypotheses*, *Annals Math. Statist.* **9** (1938) 60 [INSPIRE].

[117] H. Xu, X. Liu and T. Matsuki, *Understanding* $B^- \to X(3823)K^-$ *via rescattering mechanism and predicting* $B^- \to \eta_{c2}(^1D_2)/\psi_3(^3D_3)K^-$, *Phys. Rev. D* **94** (2016) 034005 [arXiv:1605.04776] [INSPIRE].

[118] BESIII collaboration, *Observation of* $e^+e^- \to \eta J/\psi$ *at center-of-mass energy* $\sqrt{s} = 4.009$ *GeV*, *Phys. Rev. D* **86** (2012) 071101 [arXiv:1208.1857] [INSPIRE].

[119] LHCb collaboration, *Observation of a resonance in* $B^+ \to K^+\mu^+\mu^-$ *decays at low recoil*, *Phys. Rev. Lett.* **111** (2013) 112003 [arXiv:1307.7595] [INSPIRE].

[120] BES collaboration, *Determination of the* $\psi(3770)$, $\psi(4040)$, $\psi(4160)$ *and* $\psi(4415)$ *resonance parameters*, *eConf* **C 070805** (2007) 02 [arXiv:0705.4500] [INSPIRE].

[121] LHCb collaboration, *Amplitude analysis of the* $B^+ \to D^+D^-K^+$ *decay*, *Phys. Rev. D* **102** (2020) 112003 [arXiv:2009.00026] [INSPIRE].

JHEP04(2022)046

The LHCb collaboration

R. Aaij,[32] A.S.W. Abdelmotteleb,[56] C. Abellán Beteta,[50] F. Abudinén,[56] T. Ackernley,[60] B. Adeva,[46] M. Adinolfi,[54] H. Afsharnia,[9] C. Agapopoulou,[13] C.A. Aidala,[87] S. Aiola,[25] Z. Ajaltouni,[9] S. Akar,[65] J. Albrecht,[15] F. Alessio,[48] M. Alexander,[59] A. Alfonso Albero,[45] Z. Aliouche,[62] G. Alkhazov,[38] P. Alvarez Cartelle,[55] S. Amato,[2] J.L. Amey,[54] Y. Amhis,[11] L. An,[48] L. Anderlini,[22] M. Andersson,[50] A. Andreianov,[38] M. Andreotti,[21] D. Ao,[6] F. Archilli,[17] A. Artamonov,[44] M. Artuso,[68] K. Arzymatov,[42] E. Aslanides,[10] M. Atzeni,[50] B. Audurier,[12] S. Bachmann,[17] M. Bachmayer,[49] J.J. Back,[56] P. Baladron Rodriguez,[46] V. Balagura,[12] W. Baldini,[21] J. Baptista de Souza Leite,[1] M. Barbetti,[22,h] R.J. Barlow,[62] S. Barsuk,[11] W. Barter,[61] M. Bartolini,[55] F. Baryshnikov,[83] J.M. Basels,[14] G. Bassi,[29] B. Batsukh,[4] A. Battig,[15] A. Bay,[49] A. Beck,[56] M. Becker,[15] F. Bedeschi,[29] I. Bediaga,[1] A. Beiter,[68] V. Belavin,[42] S. Belin,[27] V. Bellee,[50] K. Belous,[44] I. Belov,[40] I. Belyaev,[41] G. Bencivenni,[23] E. Ben-Haim,[13] A. Berezhnoy,[40] R. Bernet,[50] D. Berninghoff,[17] H.C. Bernstein,[68] C. Bertella,[62] A. Bertolin,[28] C. Betancourt,[50] F. Betti,[48] Ia. Bezshyiko,[50] S. Bhasin,[54] J. Bhom,[35] L. Bian,[73] M.S. Bieker,[15] N.V. Biesuz,[21] S. Bifani,[53] P. Billoir,[13] A. Biolchini,[32] M. Birch,[61] F.C.R. Bishop,[55] A. Bitadze,[62] A. Bizzeti,[22,l] M. Bjørn,[63] M.P. Blago,[55] T. Blake,[56] F. Blanc,[49] S. Blusk,[68] D. Bobulska,[59] J.A. Boelhauve,[15] O. Boente Garcia,[46] T. Boettcher,[65] O. Boiarkina,[41] A. Boldyrev,[82] A. Bondar,[43] N. Bondar,[38,48] S. Borghi,[62] M. Borisyak,[42] M. Borsato,[17] J.T. Borsuk,[35] S.A. Bouchiba,[49] T.J.V. Bowcock,[60,48] A. Boyer,[48] C. Bozzi,[21] M.J. Bradley,[61] S. Braun,[66] A. Brea Rodriguez,[46] J. Brodzicka,[35] A. Brossa Gonzalo,[56] D. Brundu,[27] A. Buonaura,[50] L. Buonincontri,[28] A.T. Burke,[62] C. Burr,[48] A. Bursche,[72] A. Butkevich,[39] J.S. Butter,[32] J. Buytaert,[48] W. Byczynski,[48] S. Cadeddu,[27] H. Cai,[73] R. Calabrese,[21,g] L. Calefice,[15,13] S. Cali,[23] R. Calladine,[53] M. Calvi,[26,k] M. Calvo Gomez,[85] P. Camargo Magalhaes,[54] P. Campana,[23] A.F. Campoverde Quezada,[6] S. Capelli,[26,k] L. Capriotti,[20,e] A. Carbone,[20,e] G. Carboni,[31,q] R. Cardinale,[24,i] A. Cardini,[27] I. Carli,[4] P. Carniti,[26,k] L. Carus,[14] K. Carvalho Akiba,[32] A. Casais Vidal,[46] R. Caspary,[17] G. Casse,[60] M. Cattaneo,[48] G. Cavallero,[48] S. Celani,[49] J. Cerasoli,[10] D. Cervenkov,[63] A.J. Chadwick,[60] M.G. Chapman,[54] M. Charles,[13] Ph. Charpentier,[48] C.A. Chavez Barajas,[60] M. Chefdeville,[8] C. Chen,[3] S. Chen,[4] A. Chernov,[35] V. Chobanova,[46] S. Cholak,[49] M. Chrzaszcz,[35] A. Chubykin,[38] V. Chulikov,[38] P. Ciambrone,[23] M.F. Cicala,[56] X. Cid Vidal,[46] G. Ciezarek,[48] P.E.L. Clarke,[58] M. Clemencic,[48] H.V. Cliff,[55] J. Closier,[48] J.L. Cobbledick,[62] V. Coco,[48] J.A.B. Coelho,[11] J. Cogan,[10] E. Cogneras,[9] L. Cojocariu,[37] P. Collins,[48] T. Colombo,[48] L. Congedo,[19,d] A. Contu,[27] N. Cooke,[53] G. Coombs,[59] I. Corredoira,[46] G. Corti,[48] C.M. Costa Sobral,[56] B. Couturier,[48] D.C. Craik,[64] J. Crkovská,[67] M. Cruz Torres,[1] R. Currie,[58] C.L. Da Silva,[67] S. Dadabaev,[83] L. Dai,[71] E. Dall'Occo,[15] J. Dalseno,[46] C. D'Ambrosio,[48] A. Danilina,[41] P. d'Argent,[48] A. Dashkina,[83] J.E. Davies,[62] A. Davis,[62] O. De Aguiar Francisco,[62] K. De Bruyn,[79] S. De Capua,[62] M. De Cian,[49] U. De Freitas Carneiro Da Graca,[1] E. De Lucia,[23] J.M. De Miranda,[1] L. De Paula,[2] M. De Serio,[19,d] D. De Simone,[50] P. De Simone,[23] F. De Vellis,[15] J.A. de Vries,[80] C.T. Dean,[67] F. Debernardis,[19,d] D. Decamp,[8] V. Dedu,[10] L. Del Buono,[13] B. Delaney,[55] H.-P. Dembinski,[15] V. Denysenko,[50] D. Derkach,[82] O. Deschamps,[9] F. Dettori,[27,f] B. Dey,[77] A. Di Cicco,[23] P. Di Nezza,[23] S. Didenko,[83] L. Dieste Maronas,[46] H. Dijkstra,[48] S. Ding,[68] V. Dobishuk,[52] C. Dong,[3] A.M. Donohoe,[18] F. Dordei,[27] A.C. dos Reis,[1] L. Douglas,[59] A. Dovbnya,[51] A.G. Downes,[8] M.W. Dudek,[35] L. Dufour,[48] V. Duk,[78] P. Durante,[48] J.M. Durham,[67] D. Dutta,[62] A. Dziurda,[35] A. Dzyuba,[38] S. Easo,[57] U. Egede,[69] V. Egorychev,[41] S. Eidelman,[43,u,†] S. Eisenhardt,[58] S. Ek-In,[49] L. Eklund,[86] S. Ely,[68] A. Ene,[37] E. Epple,[67] S. Escher,[14] J. Eschle,[50] S. Esen,[50] T. Evans,[62] L.N. Falcao,[1] Y. Fan,[6] B. Fang,[73]

JHEP04(2022)046

S. Farry,[60] D. Fazzini,[26,k] M. Féo,[48] A. Fernandez Prieto,[46] A.D. Fernez,[66] F. Ferrari,[20] L. Ferreira Lopes,[49] F. Ferreira Rodrigues,[2] S. Ferreres Sole,[32] M. Ferrillo,[50] M. Ferro-Luzzi,[48] S. Filippov,[39] R.A. Fini,[19] M. Fiorini,[21,g] M. Firlej,[34] K.M. Fischer,[63] D.S. Fitzgerald,[87] C. Fitzpatrick,[62] T. Fiutowski,[34] A. Fkiaras,[48] F. Fleuret,[12] M. Fontana,[13] F. Fontanelli,[24,i] R. Forty,[48] D. Foulds-Holt,[55] V. Franco Lima,[60] M. Franco Sevilla,[66] M. Frank,[48] E. Franzoso,[21] G. Frau,[17] C. Frei,[48] D.A. Friday,[59] J. Fu,[6] Q. Fuehring,[15] E. Gabriel,[32] G. Galati,[19,d] A. Gallas Torreira,[46] D. Galli,[20,e] S. Gambetta,[58,48] Y. Gan,[3] M. Gandelman,[2] P. Gandini,[25] Y. Gao,[5] M. Garau,[27] L.M. Garcia Martin,[56] P. Garcia Moreno,[45] J. García Pardiñas,[26,k] B. Garcia Plana,[46] F.A. Garcia Rosales,[12] L. Garrido,[45] C. Gaspar,[48] R.E. Geertsema,[32] D. Gerick,[17] L.L. Gerken,[15] E. Gersabeck,[62] M. Gersabeck,[62] T. Gershon,[56] D. Gerstel,[10] L. Giambastiani,[28] V. Gibson,[55] H.K. Giemza,[36] A.L. Gilman,[63] M. Giovannetti,[23,q] A. Gioventù,[46] P. Gironella Gironell,[45] C. Giugliano,[21] K. Gizdov,[58] E.L. Gkougkousis,[48] V.V. Gligorov,[13,48] C. Göbel,[70] E. Golobardes,[85] D. Golubkov,[41] A. Golutvin,[61,83] A. Gomes,[1,a] S. Gomez Fernandez,[45] F. Goncalves Abrantes,[63] M. Goncerz,[35] G. Gong,[3] P. Gorbounov,[41] I.V. Gorelov,[40] C. Gotti,[26] J.P. Grabowski,[17] T. Grammatico,[13] L.A. Granado Cardoso,[48] E. Graugés,[45] E. Graverini,[49] G. Graziani,[22] A. Grecu,[37] L.M. Greeven,[32] N.A. Grieser,[4] L. Grillo,[62] S. Gromov,[83] B.R. Gruberg Cazon,[63] C. Gu,[3] M. Guarise,[21] M. Guittiere,[11] P.A. Günther,[17] E. Gushchin,[39] A. Guth,[14] Y. Guz,[44] T. Gys,[48] T. Hadavizadeh,[69] G. Haefeli,[49] C. Haen,[48] J. Haimberger,[48] S.C. Haines,[55] T. Halewood-leagas,[60] P.M. Hamilton,[66] J.P. Hammerich,[60] Q. Han,[7] X. Han,[17] E.B. Hansen,[62] S. Hansmann-Menzemer,[17] N. Harnew,[63] T. Harrison,[60] C. Hasse,[48] M. Hatch,[48] J. He,[6,b] M. Hecker,[61] K. Heijhoff,[32] K. Heinicke,[15] R.D.L. Henderson,[69,56] A.M. Hennequin,[48] K. Hennessy,[60] L. Henry,[48] J. Heuel,[14] A. Hicheur,[2] D. Hill,[49] M. Hilton,[62] S.E. Hollitt,[15] R. Hou,[7] Y. Hou,[8] J. Hu,[17] J. Hu,[72] W. Hu,[7] X. Hu,[3] W. Huang,[6] X. Huang,[73] W. Hulsbergen,[32] R.J. Hunter,[56] M. Hushchyn,[82] D. Hutchcroft,[60] D. Hynds,[32] P. Ibis,[15] M. Idzik,[34] D. Ilin,[38] P. Ilten,[65] A. Inglessi,[38] A. Ishteev,[83] K. Ivshin,[38] R. Jacobsson,[48] H. Jage,[14] S. Jakobsen,[48] E. Jans,[32] B.K. Jashal,[47] A. Jawahery,[66] V. Jevtic,[15] X. Jiang,[4] M. John,[63] D. Johnson,[64] C.R. Jones,[55] T.P. Jones,[56] B. Jost,[48] N. Jurik,[48] S. Kandybei,[51] Y. Kang,[3] M. Karacson,[48] D. Karpenkov,[83] M. Karpov,[82] J.W. Kautz,[65] F. Keizer,[48] D.M. Keller,[68] M. Kenzie,[56] T. Ketel,[33] B. Khanji,[15] A. Kharisova,[84] S. Kholodenko,[44] T. Kirn,[14] V.S. Kirsebom,[49] O. Kitouni,[64] S. Klaver,[33] N. Kleijne,[29] K. Klimaszewski,[36] M.R. Kmiec,[36] S. Koliiev,[52] A. Kondybayeva,[83] A. Konoplyannikov,[41] P. Kopciewicz,[34] R. Kopecna,[17] P. Koppenburg,[32] M. Korolev,[40] I. Kostiuk,[32,52] O. Kot,[52] S. Kotriakhova,[21,38] A. Kozachuk,[40] P. Kravchenko,[38] L. Kravchuk,[39] R.D. Krawczyk,[48] M. Kreps,[56] S. Kretzschmar,[14] P. Krokovny,[43,u] W. Krupa,[34] W. Krzemien,[36] J. Kubat,[17] M. Kucharczyk,[35] V. Kudryavtsev,[43,u] H.S. Kuindersma,[32,33] G.J. Kunde,[67] T. Kvaratskheliya,[41] D. Lacarrere,[48] G. Lafferty,[62] A. Lai,[27] A. Lampis,[27] D. Lancierini,[50] J.J. Lane,[62] R. Lane,[54] G. Lanfranchi,[23] C. Langenbruch,[14] J. Langer,[15] O. Lantwin,[83] T. Latham,[56] F. Lazzari,[29] R. Le Gac,[10] S.H. Lee,[87] R. Lefèvre,[9] A. Leflat,[40] S. Legotin,[83] O. Leroy,[10] T. Lesiak,[35] B. Leverington,[17] H. Li,[72] P. Li,[17] S. Li,[7] Y. Li,[4] Z. Li,[68] X. Liang,[68] T. Lin,[61] R. Lindner,[48] V. Lisovskyi,[15] R. Litvinov,[27] G. Liu,[72] H. Liu,[6] Q. Liu,[6] S. Liu,[4] A. Lobo Salvia,[45] A. Loi,[27] R. Lollini,[78] J. Lomba Castro,[46] I. Longstaff,[59] J.H. Lopes,[2] S. López Soliño,[46] G.H. Lovell,[55] Y. Lu,[4] C. Lucarelli,[22,h] D. Lucchesi,[28,m] S. Luchuk,[39] M. Lucio Martinez,[32] V. Lukashenko,[32,52] Y. Luo,[3] A. Lupato,[62] E. Luppi,[21,g] O. Lupton,[56] A. Lusiani,[29,n] X. Lyu,[6] L. Ma,[4] R. Ma,[6] S. Maccolini,[20] F. Machefert,[11] F. Maciuc,[37] V. Macko,[49] P. Mackowiak,[15] S. Maddrell-Mander,[54] L.R. Madhan Mohan,[54] O. Maev,[38] A. Maevskiy,[82] D. Maisuzenko,[38] M.W. Majewski,[34] J.J. Malczewski,[35] S. Malde,[63] B. Malecki,[35] A. Malinin,[81] T. Maltsev,[43,u] H. Malygina,[17] G. Manca,[27,f] G. Mancinelli,[10] D. Manuzzi,[20] D. Marangotto,[25,j] J. Maratas,[9,s] J.F. Marchand,[8] U. Marconi,[20] S. Mariani,[22,h] C. Marin Benito,[48] M. Marinangeli,[49] J. Marks,[17]

JHEP04(2022)046

A.M. Marshall,[54] P.J. Marshall,[60] G. Martelli,[78] G. Martellotti,[30] L. Martinazzoli,[48,k] M. Martinelli,[26,k] D. Martinez Santos,[46] F. Martinez Vidal,[47] A. Massafferri,[1] M. Materok,[14] R. Matev,[48] A. Mathad,[50] V. Matiunin,[41] C. Matteuzzi,[26] K.R. Mattioli,[87] A. Mauri,[32] E. Maurice,[12] J. Mauricio,[45] M. Mazurek,[48] M. McCann,[61] L. Mcconnell,[18] T.H. Mcgrath,[62] N.T. Mchugh,[59] A. McNab,[62] R. McNulty,[18] J.V. Mead,[60] B. Meadows,[65] G. Meier,[15] D. Melnychuk,[36] S. Meloni,[26,k] M. Merk,[32,80] A. Merli,[25,j] L. Meyer Garcia,[2] M. Mikhasenko,[75,c] D.A. Milanes,[74] E. Millard,[56] M. Milovanovic,[48] M.-N. Minard,[8] A. Minotti,[26,k] S.E. Mitchell,[58] B. Mitreska,[62] D.S. Mitzel,[15] A. Mödden,[15] R.A. Mohammed,[63] R.D. Moise,[61] S. Mokhnenko,[82] T. Mombächer,[46] I.A. Monroy,[74] S. Monteil,[9] M. Morandin,[28] G. Morello,[23] M.J. Morello,[29,n] J. Moron,[34] A.B. Morris,[75] A.G. Morris,[56] R. Mountain,[68] H. Mu,[3] F. Muheim,[58] M. Mulder,[79] K. Müller,[50] C.H. Murphy,[63] D. Murray,[62] R. Murta,[61] P. Muzzetto,[27] P. Naik,[54] T. Nakada,[49] R. Nandakumar,[57] T. Nanut,[48] I. Nasteva,[2] M. Needham,[58] N. Neri,[25,j] S. Neubert,[75] N. Neufeld,[48] R. Newcombe,[61] E.M. Niel,[49] S. Nieswand,[14] N. Nikitin,[40] N.S. Nolte,[64] C. Normand,[8] C. Nunez,[87] A. Oblakowska-Mucha,[34] V. Obraztsov,[44] T. Oeser,[14] D.P. O'Hanlon,[54] S. Okamura,[21] R. Oldeman,[27,f] F. Oliva,[58] M.E. Olivares,[68] C.J.G. Onderwater,[79] R.H. O'Neil,[58] J.M. Otalora Goicochea,[2] T. Ovsiannikova,[41] P. Owen,[50] A. Oyanguren,[47] O. Ozcelik,[58] K.O. Padeken,[75] B. Pagare,[56] P.R. Pais,[48] T. Pajero,[63] A. Palano,[19] M. Palutan,[23] Y. Pan,[62] G. Panshin,[84] A. Papanestis,[57] M. Pappagallo,[19,d] L.L. Pappalardo,[21,g] C. Pappenheimer,[65] W. Parker,[66] C. Parkes,[62] B. Passalacqua,[21] G. Passaleva,[22] A. Pastore,[19] M. Patel,[61] C. Patrignani,[20,e] C.J. Pawley,[80] A. Pearce,[48,57] A. Pellegrino,[32] M. Pepe Altarelli,[48] S. Perazzini,[20] D. Pereima,[41] A. Pereiro Castro,[46] P. Perret,[9] M. Petric,[59,48] K. Petridis,[54] A. Petrolini,[24,i] A. Petrov,[81] S. Petrucci,[58] M. Petruzzo,[25] T.T.H. Pham,[68] A. Philippov,[42] R. Piandani,[6] L. Pica,[29,n] M. Piccini,[78] B. Pietrzyk,[8] G. Pietrzyk,[11] M. Pili,[63] D. Pinci,[30] F. Pisani,[48] M. Pizzichemi,[26,48,k] P.K. Resmi,[10] V. Placinta,[37] J. Plews,[53] M. Plo Casasus,[46] F. Polci,[13,48] M. Poli Lener,[23] M. Poliakova,[68] A. Poluektov,[10] N. Polukhina,[83,t] I. Polyakov,[68] E. Polycarpo,[2] S. Ponce,[48] D. Popov,[6,48] S. Popov,[42] S. Poslavskii,[44] K. Prasanth,[35] L. Promberger,[48] C. Prouve,[46] V. Pugatch,[52] V. Puill,[11] G. Punzi,[29,o] H. Qi,[3] W. Qian,[6] N. Qin,[3] R. Quagliani,[49] N.V. Raab,[18] R.I. Rabadan Trejo,[6] B. Rachwal,[34] J.H. Rademacker,[54] R. Rajagopalan,[68] M. Rama,[29] M. Ramos Pernas,[56] M.S. Rangel,[2] F. Ratnikov,[42,82] G. Raven,[33,48] M. Reboud,[8] F. Redi,[48] F. Reiss,[62] C. Remon Alepuz,[47] Z. Ren,[3] V. Renaudin,[63] R. Ribatti,[29] A.M. Ricci,[27] S. Ricciardi,[57] K. Rinnert,[60] P. Robbe,[11] G. Robertson,[58] A.B. Rodrigues,[49] E. Rodrigues,[60] J.A. Rodriguez Lopez,[74] E.R.R. Rodriguez Rodriguez,[46] A. Rollings,[63] P. Roloff,[48] V. Romanovskiy,[44] M. Romero Lamas,[46] A. Romero Vidal,[46] J.D. Roth,[87] M. Rotondo,[23] M.S. Rudolph,[68] T. Ruf,[48] R.A. Ruiz Fernandez,[46] J. Ruiz Vidal,[47] A. Ryzhikov,[82] J. Ryzka,[34] J.J. Saborido Silva,[46] N. Sagidova,[38] N. Sahoo,[53] B. Saitta,[27,f] M. Salomoni,[48] C. Sanchez Gras,[32] R. Santacesaria,[30] C. Santamarina Rios,[46] M. Santimaria,[23] E. Santovetti,[31,q] D. Saranin,[83] G. Sarpis,[14] M. Sarpis,[75] A. Sarti,[30] C. Satriano,[30,p] A. Satta,[31] M. Saur,[15] D. Savrina,[41,40] H. Sazak,[9] L.G. Scantlebury Smead,[63] A. Scarabotto,[13] S. Schael,[14] S. Scherl,[60] M. Schiller,[59] H. Schindler,[48] M. Schmelling,[16] B. Schmidt,[48] S. Schmitt,[14] O. Schneider,[49] A. Schopper,[48] M. Schubiger,[32] S. Schulte,[49] M.H. Schune,[11] R. Schwemmer,[48] B. Sciascia,[23,48] S. Sellam,[46] A. Semennikov,[41] M. Senghi Soares,[33] A. Sergi,[24,i] N. Serra,[50] L. Sestini,[28] A. Seuthe,[15] Y. Shang,[5] D.M. Shangase,[87] M. Shapkin,[44] I. Shchemerov,[83] L. Shchutska,[49] T. Shears,[60] L. Shekhtman,[43,u] Z. Shen,[5] S. Sheng,[4] V. Shevchenko,[81] E.B. Shields,[26,k] Y. Shimizu,[11] E. Shmanin,[83] J.D. Shupperd,[68] B.G. Siddi,[21] R. Silva Coutinho,[50] G. Simi,[28] S. Simone,[19,d] N. Skidmore,[62] R. Skuza,[17] T. Skwarnicki,[68] M.W. Slater,[53] I. Slazyk,[21,g] J.C. Smallwood,[63] J.G. Smeaton,[55] E. Smith,[50] M. Smith,[61] A. Snoch,[32] L. Soares Lavra,[9] M.D. Sokoloff,[65] F.J.P. Soler,[59] A. Solovev,[38] I. Solovyev,[38] F.L. Souza De Almeida,[2]

JHEP04(2022)046

B. Souza De Paula,[2] B. Spaan,[15] E. Spadaro Norella,[25,j] P. Spradlin,[59] F. Stagni,[48] M. Stahl,[65] S. Stahl,[48] S. Stanislaus,[63] O. Steinkamp,[50,83] O. Stenyakin,[44] H. Stevens,[15] S. Stone,[68,48,†] D. Strekalina,[83] F. Suljik,[63] J. Sun,[27] L. Sun,[73] Y. Sun,[66] P. Svihra,[62] P.N. Swallow,[53] K. Swientek,[34] A. Szabelski,[36] T. Szumlak,[34] M. Szymanski,[48] S. Taneja,[62] A.R. Tanner,[54] M.D. Tat,[63] A. Terentev,[83] F. Teubert,[48] E. Thomas,[48] D.J.D. Thompson,[53] K.A. Thomson,[60] H. Tilquin,[61] V. Tisserand,[9] S. T'Jampens,[8] M. Tobin,[4] L. Tomassetti,[21,g] X. Tong,[5] D. Torres Machado,[1] D.Y. Tou,[3] E. Trifonova,[83] S.M. Trilov,[54] C. Trippl,[49] G. Tuci,[6] A. Tully,[49] N. Tuning,[32,48] A. Ukleja,[36,48] D.J. Unverzagt,[17] E. Ursov,[83] A. Usachov,[32] A. Ustyuzhanin,[42,82] U. Uwer,[17] A. Vagner,[84] V. Vagnoni,[20] A. Valassi,[48] G. Valenti,[20] N. Valls Canudas,[85] M. van Beuzekom,[32] M. Van Dijk,[49] H. Van Hecke,[67] E. van Herwijnen,[83] M. van Veghel,[79] R. Vazquez Gomez,[45] P. Vazquez Regueiro,[46] C. Vázquez Sierra,[48] S. Vecchi,[21] J.J. Velthuis,[54] M. Veltri,[22,r] A. Venkateswaran,[68] M. Veronesi,[32] M. Vesterinen,[56] D. Vieira,[65] M. Vieites Diaz,[49] H. Viemann,[76] X. Vilasis-Cardona,[85] E. Vilella Figueras,[60] A. Villa,[20] P. Vincent,[13] F.C. Volle,[11] D. Vom Bruch,[10] A. Vorobyev,[38] V. Vorobyev,[43,u] N. Voropaev,[38] K. Vos,[80] R. Waldi,[17] J. Walsh,[29] C. Wang,[17] J. Wang,[5] J. Wang,[4] J. Wang,[3] J. Wang,[73] M. Wang,[3] R. Wang,[54] Y. Wang,[7] Z. Wang,[50] Z. Wang,[3] Z. Wang,[6] J.A. Ward,[56,69] N.K. Watson,[53] D. Websdale,[61] C. Weisser,[64] B.D.C. Westhenry,[54] D.J. White,[62] M. Whitehead,[54] A.R. Wiederhold,[56] D. Wiedner,[15] G. Wilkinson,[63] M.K. Wilkinson,[68] I. Williams,[55] M. Williams,[64] M.R.J. Williams,[58] F.F. Wilson,[57] W. Wislicki,[36] M. Witek,[35] L. Witola,[17] G. Wormser,[11] S.A. Wotton,[55] H. Wu,[68] K. Wyllie,[48] Z. Xiang,[6] D. Xiao,[7] Y. Xie,[7] A. Xu,[5] J. Xu,[6] L. Xu,[3] M. Xu,[56] Q. Xu,[6] Z. Xu,[9] Z. Xu,[6] D. Yang,[3] S. Yang,[6] Y. Yang,[6] Z. Yang,[5] Z. Yang,[66] Y. Yao,[68] L.E. Yeomans,[60] H. Yin,[7] J. Yu,[71] X. Yuan,[68] O. Yushchenko,[44] E. Zaffaroni,[49] M. Zavertyaev,[16,t] M. Zdybal,[35] O. Zenaiev,[48] M. Zeng,[3] D. Zhang,[7] L. Zhang,[3] S. Zhang,[71] S. Zhang,[5] Y. Zhang,[5] Y. Zhang,[63] A. Zharkova,[83] A. Zhelezov,[17] Y. Zheng,[6] T. Zhou,[5] X. Zhou,[6] Y. Zhou,[6] V. Zhovkovska,[11] X. Zhu,[3] X. Zhu,[7] Z. Zhu,[6] V. Zhukov,[14,40] Q. Zou,[4] S. Zucchelli,[20,e] D. Zuliani,[28] G. Zunica[62]

[1] *Centro Brasileiro de Pesquisas Físicas (CBPF), Rio de Janeiro, Brazil*
[2] *Universidade Federal do Rio de Janeiro (UFRJ), Rio de Janeiro, Brazil*
[3] *Center for High Energy Physics, Tsinghua University, Beijing, China*
[4] *Institute Of High Energy Physics (IHEP), Beijing, China*
[5] *School of Physics State Key Laboratory of Nuclear Physics and Technology, Peking University, Beijing, China*
[6] *University of Chinese Academy of Sciences, Beijing, China*
[7] *Institute of Particle Physics, Central China Normal University, Wuhan, Hubei, China*
[8] *Univ. Savoie Mont Blanc, CNRS, IN2P3-LAPP, Annecy, France*
[9] *Université Clermont Auvergne, CNRS/IN2P3, LPC, Clermont-Ferrand, France*
[10] *Aix Marseille Univ, CNRS/IN2P3, CPPM, Marseille, France*
[11] *Université Paris-Saclay, CNRS/IN2P3, IJCLab, Orsay, France*
[12] *Laboratoire Leprince-Ringuet, CNRS/IN2P3, Ecole Polytechnique, Institut Polytechnique de Paris, Palaiseau, France*
[13] *LPNHE, Sorbonne Université, Paris Diderot Sorbonne Paris Cité, CNRS/IN2P3, Paris, France*
[14] *I. Physikalisches Institut, RWTH Aachen University, Aachen, Germany*
[15] *Fakultät Physik, Technische Universität Dortmund, Dortmund, Germany*
[16] *Max-Planck-Institut für Kernphysik (MPIK), Heidelberg, Germany*
[17] *Physikalisches Institut, Ruprecht-Karls-Universität Heidelberg, Heidelberg, Germany*
[18] *School of Physics, University College Dublin, Dublin, Ireland*
[19] *INFN Sezione di Bari, Bari, Italy*
[20] *INFN Sezione di Bologna, Bologna, Italy*
[21] *INFN Sezione di Ferrara, Ferrara, Italy*

JHEP04(2022)046

[22] *INFN Sezione di Firenze, Firenze, Italy*
[23] *INFN Laboratori Nazionali di Frascati, Frascati, Italy*
[24] *INFN Sezione di Genova, Genova, Italy*
[25] *INFN Sezione di Milano, Milano, Italy*
[26] *INFN Sezione di Milano-Bicocca, Milano, Italy*
[27] *INFN Sezione di Cagliari, Monserrato, Italy*
[28] *Universita degli Studi di Padova, Universita e INFN, Padova, Padova, Italy*
[29] *INFN Sezione di Pisa, Pisa, Italy*
[30] *INFN Sezione di Roma La Sapienza, Roma, Italy*
[31] *INFN Sezione di Roma Tor Vergata, Roma, Italy*
[32] *Nikhef National Institute for Subatomic Physics, Amsterdam, Netherlands*
[33] *Nikhef National Institute for Subatomic Physics and VU University Amsterdam, Amsterdam, Netherlands*
[34] *AGH — University of Science and Technology, Faculty of Physics and Applied Computer Science, Kraków, Poland*
[35] *Henryk Niewodniczanski Institute of Nuclear Physics Polish Academy of Sciences, Kraków, Poland*
[36] *National Center for Nuclear Research (NCBJ), Warsaw, Poland*
[37] *Horia Hulubei National Institute of Physics and Nuclear Engineering, Bucharest-Magurele, Romania*
[38] *Petersburg Nuclear Physics Institute NRC Kurchatov Institute (PNPI NRC KI), Gatchina, Russia*
[39] *Institute for Nuclear Research of the Russian Academy of Sciences (INR RAS), Moscow, Russia*
[40] *Institute of Nuclear Physics, Moscow State University (SINP MSU), Moscow, Russia*
[41] *Institute of Theoretical and Experimental Physics NRC Kurchatov Institute (ITEP NRC KI), Moscow, Russia*
[42] *Yandex School of Data Analysis, Moscow, Russia*
[43] *Budker Institute of Nuclear Physics (SB RAS), Novosibirsk, Russia*
[44] *Institute for High Energy Physics NRC Kurchatov Institute (IHEP NRC KI), Protvino, Russia, Protvino, Russia*
[45] *ICCUB, Universitat de Barcelona, Barcelona, Spain*
[46] *Instituto Galego de Física de Altas Enerxías (IGFAE), Universidade de Santiago de Compostela, Santiago de Compostela, Spain*
[47] *Instituto de Fisica Corpuscular, Centro Mixto Universidad de Valencia — CSIC, Valencia, Spain*
[48] *European Organization for Nuclear Research (CERN), Geneva, Switzerland*
[49] *Institute of Physics, Ecole Polytechnique Fédérale de Lausanne (EPFL), Lausanne, Switzerland*
[50] *Physik-Institut, Universität Zürich, Zürich, Switzerland*
[51] *NSC Kharkiv Institute of Physics and Technology (NSC KIPT), Kharkiv, Ukraine*
[52] *Institute for Nuclear Research of the National Academy of Sciences (KINR), Kyiv, Ukraine*
[53] *University of Birmingham, Birmingham, United Kingdom*
[54] *H.H. Wills Physics Laboratory, University of Bristol, Bristol, United Kingdom*
[55] *Cavendish Laboratory, University of Cambridge, Cambridge, United Kingdom*
[56] *Department of Physics, University of Warwick, Coventry, United Kingdom*
[57] *STFC Rutherford Appleton Laboratory, Didcot, United Kingdom*
[58] *School of Physics and Astronomy, University of Edinburgh, Edinburgh, United Kingdom*
[59] *School of Physics and Astronomy, University of Glasgow, Glasgow, United Kingdom*
[60] *Oliver Lodge Laboratory, University of Liverpool, Liverpool, United Kingdom*
[61] *Imperial College London, London, United Kingdom*
[62] *Department of Physics and Astronomy, University of Manchester, Manchester, United Kingdom*
[63] *Department of Physics, University of Oxford, Oxford, United Kingdom*
[64] *Massachusetts Institute of Technology, Cambridge, MA, United States*
[65] *University of Cincinnati, Cincinnati, OH, United States*
[66] *University of Maryland, College Park, MD, United States*
[67] *Los Alamos National Laboratory (LANL), Los Alamos, United States*
[68] *Syracuse University, Syracuse, NY, United States*

JHEP04(2022)046

[69] School of Physics and Astronomy, Monash University, Melbourne, Australia, associated to [56]
[70] Pontifícia Universidade Católica do Rio de Janeiro (PUC-Rio), Rio de Janeiro, Brazil, associated to [2]
[71] Physics and Micro Electronic College, Hunan University, Changsha City, China, associated to [7]
[72] Guangdong Provincial Key Laboratory of Nuclear Science, Guangdong-Hong Kong Joint Laboratory of Quantum Matter, Institute of Quantum Matter, South China Normal University, Guangzhou, China, associated to [3]
[73] School of Physics and Technology, Wuhan University, Wuhan, China, associated to [3]
[74] Departamento de Fisica, Universidad Nacional de Colombia, Bogota, Colombia, associated to [13]
[75] Universität Bonn — Helmholtz-Institut für Strahlen und Kernphysik, Bonn, Germany, associated to [17]
[76] Institut für Physik, Universität Rostock, Rostock, Germany, associated to [17]
[77] Eotvos Lorand University, Budapest, Hungary, associated to [48]
[78] INFN Sezione di Perugia, Perugia, Italy, associated to [21]
[79] Van Swinderen Institute, University of Groningen, Groningen, Netherlands, associated to [32]
[80] Universiteit Maastricht, Maastricht, Netherlands, associated to [32]
[81] National Research Centre Kurchatov Institute, Moscow, Russia, associated to [41]
[82] National Research University Higher School of Economics, Moscow, Russia, associated to [42]
[83] National University of Science and Technology "MISIS", Moscow, Russia, associated to [41]
[84] National Research Tomsk Polytechnic University, Tomsk, Russia, associated to [41]
[85] DS4DS, La Salle, Universitat Ramon Llull, Barcelona, Spain, associated to [45]
[86] Department of Physics and Astronomy, Uppsala University, Uppsala, Sweden, associated to [59]
[87] University of Michigan, Ann Arbor, United States, associated to [68]

[a] Universidade Federal do Triângulo Mineiro (UFTM), Uberaba-MG, Brazil
[b] Hangzhou Institute for Advanced Study, UCAS, Hangzhou, China
[c] Excellence Cluster ORIGINS, Munich, Germany
[d] Università di Bari, Bari, Italy
[e] Università di Bologna, Bologna, Italy
[f] Università di Cagliari, Cagliari, Italy
[g] Università di Ferrara, Ferrara, Italy
[h] Università di Firenze, Firenze, Italy
[i] Università di Genova, Genova, Italy
[j] Università degli Studi di Milano, Milano, Italy
[k] Università di Milano Bicocca, Milano, Italy
[l] Università di Modena e Reggio Emilia, Modena, Italy
[m] Università di Padova, Padova, Italy
[n] Scuola Normale Superiore, Pisa, Italy
[o] Università di Pisa, Pisa, Italy
[p] Università della Basilicata, Potenza, Italy
[q] Università di Roma Tor Vergata, Roma, Italy
[r] Università di Urbino, Urbino, Italy
[s] MSU — Iligan Institute of Technology (MSU-IIT), Iligan, Philippines
[t] P.N. Lebedev Physical Institute, Russian Academy of Science (LPI RAS), Moscow, Russia
[u] Novosibirsk State University, Novosibirsk, Russia
[†] Deceased

JHEP04(2022)046